Structure-related Effects of Pentosan Polysulfate Sodium: Modulation on Phenotypic Change and Chondrogenic Properties in Canine Chondrocyte *in-vitro* Cultures

（ポリ硫酸ペントサンの構造と効果発現に関する研究：
培養軟骨細胞における形質維持と軟骨分化能の調節）

Yanlin Wang

HOKKAIDO UNIVERSITY

Structure-related Effects of Pentosan Polysulfate Sodium: Modulation on Phenotypic Change and Chondrogenic Properties in Canine Chondrocyte *in-vitro* Cultures

（ポリ硫酸ペントサンの構造と効果発現に関する研究：培養軟骨細胞における形質維持と軟骨分化能の調節）

A Dissertation for the Degree of Doctor of Philosophy

Yanlin Wang

Laboratory of Veterinary Surgery

Department of Veterinary Clinical Sciences

Graduate School of Veterinary Medicine

2023

Dissertation Examination Committee:

Professor Masahiro Okumura, Supervisor

Professor Takashi Kimura

Associate Professor Osamu Ichii

Assistant Professor Takafumi Sunaga

Structure-related Effects of Pentosan Polysulfate Sodium: Modulation on Phenotypic Change and Chondrogenic Properties in Canine Chondrocyte *in-vitro* Cultures

by

Yanlin Wang

A dissertation submitted to the Graduate School of Veterinary Medicine of Hokkaido University in fulfillment of the requirements for the degree of Doctor of Philosophy

Hokkaido University

Japan

2023

List of Abbreviations

2D	Two-dimensional
3D	Three-dimensional
µg	Microgram
µL	Microliter
ADAMTS5	A disintegrin and metalloproteinase with thrombospondin motifs 5
Akt	Protein kinase B
ANOVA	Analysis of variance
BSA	Bovine serum albumin
CCND1	Cyclin D1
CDK	Cyclin-dependent kinase
cDNA	Complementary deoxyribonucleic acid
cm^2	Square centimeter
COL1A2	Collagen type I alpha 2 chain
COL2A1	Collagen type II alpha 1 chain
Da	Dalton
DMEM	Dulbecco's modified eagle's medium
DMOAD	Disease modifying osteoarthritic drug
DMSO	Dimethyl sulfoxide
DNA	Deoxyribonucleic acid
ECM	Extracellular matrix
EDTA	Ethylenediaminetetraacetic acid
FBS	Fetal bovine serum
FITC	Fluorescein isothiocyanate
GAPDH	Glyceraldehyde-3-phosphate dehydrogenase
HCl	Hydrogen chloride
HEPES	4-(2-hydroxyethyl)-1-piperazineethanesulfonic acid
hr	Hour

HRP	Horseradish peroxidase
mg	Milligram
min	Minute
mL	Milliliter
mm	Millimeter
mM	Millimolar
M-MLV	Murine leukemia virus reverse transcriptase
MSC	Mesenchymal stem cells
mRNA	Messenger ribonucleic acid
MTT	3-(4,5-dimehylthiazolyl-2)2,5-diphenyltetrazolium bromide
$NaHCO_3$	Sodium hydrogen carbonate
nm	Nanometer
NSAID	Nonsteroidal anti-inflammatory drug
OA	Osteoarthritis
p110α	Phosphatidylinositol 3-kinase catalytic subunit alpha
PBS	Phosphate-buffered saline
PBST	Phosphate-buffered saline with 0.1% Tween 20
PI	Propidium iodide
PI3K	Phosphatidylinositol 3-kinase
PPS	Pentosan polysulfate sodium
PVDF	Polyvinylidene difluoride
qPCR	Quantitative real-time polymerase chain reaction
RIPA	Radioimmunoprecipitation assay
RNA	Ribonucleic acid
SD	Standard deviation
SDS-PAGE	Sodium dodecyl sulfate-polyacrylamide gel electrophoresis
SOX9	SRY-Box transcription factor 9
TIMP3	Tissue inhibitor of metalloproteinases 3

Table of Contents

List of Tables

List of Figures

List of Publications Related to the Dissertation

The contents of this dissertation are based on the following original publications and submitted manuscripts under review listed below by the Roman numeral I and II of the research conducted during the period April 2019 - March 2023.

I. **Wang Y**, Mwale C, Akaraphutiporn E, Kim S, Sunaga T, Okumura M. Sulfate level relied effects of pentosan polysulfate sodium on inhibiting the proliferation of canine articular chondrocytes by targeting PI3K/Akt pathway. Jpn J Vet Res, in press.

II. **Wang Y**, Sunaga T, Mwale C, Akaraphutiporn E, Kim S, Okumura M. Pentosan polysulfate sodium promotes redifferentiation to the original phenotype in micromass-cultured canine articular chondrocytes and exerts molecular weight-dependent effects. J Vet Med Sci, in press.

General Introduction

Osteoarthritis (OA) is a common chronic degenerative joint disease that affects multiple joint structures including cartilages, synovial membranes, ligaments, and subchondral bones, and clinically characterized by chronic joint pain, stiffness, and reduced joint movement (Dequeker *et al.*, 2008; Glyn-Jones *et al.*, 2015; Loeser *et al.*, 2012). In humans, OA has affected over 500 million people of the global population in 2019, which greatly reduces the quality of life and causes 2% of the global years lived with disability in the patients and generates a socioeconomic burden (Hunter *et al.*, 2020). The prevalence of dogs with OA is vary between studies. While a previous study in the U.S.A. reported up to 20% of dogs over 1-year old are suffered from the disease (Johnston, 1997), estimated number of dogs presenting with OA has been reported up to 6.6% in the U.K (O'Neill *et al.*, 2014). In horses, around 60% of the lameness is considered to be associated with OA (Caron *et al.*, 2003), and the estimated direct and indirect financial costs for OA horses could exceed one billion dollar per year in the U.S.A. (Keegan, 2007). Thus, OA has now been recognized as a major metabolic disorder in joints with multiple etiologies in both human and veterinary medicine.

In the joint, hyaline articular cartilage is a special layer of avascular connective tissue covering the joint surface (Goldring *et al.*, 2009). Hyaline cartilage consists of 1–5% of specialized resident cells called chondrocytes embedded in the extracellular matrix (ECM) produced by chondrocytes, which are responsive to renew the components of this ECM continuously (Fox *et al.*, 2009). The major components of the cartilage include 15–20% of collagen fibers (dominantly type II collagens), 3–10% of negatively charged proteoglycans, and a large amount of water trapped by the negatively charged environment (Borthakur *et al.*, 2006; Eyre *et al.*, 1995; Fox *et al.*, 2009). This structure lets hyaline cartilage absorbs the mechanical pressure and distributes the weight over the subchondral bone, and makes normal motion of the joint be possible (Gao *et al.*, 2014; Fox *et al.*, 2009). Although ideally, articular cartilages will function through the lifetime, it could be affected by multiple risk factors, including age, traumatic injury, obesity, and genetic factors, which lead to the development and progression of OA (Glyn-Jones *et al.*, 2015; Goldring *et al.*, 2009; Sokolove *et al.*, 2013). Key events in the pathogenesis of OA of articular cartilage include an

interruption of anabolic and catabolic signals, caused by cytokines and inflammatory mediators (Kapoor, 2015; Krasnokutsky *et al.*, 2008). The biochemical changes in OA cartilage include reduced proteoglycan contents, disruption of the arrangement of the collagen type II fibril network and aggregation of proteoglycans, and upregulated synthetic activities and degradation of the ECM macromolecular components (Loeser *et al.*, 2012; Sokolove *et al.*, 2013). Water content in OA cartilage was increased firstly, then reduced with the loss of ECM components. (Loeser *et al.*, 2012). The breakdown of the ECM structures leads to changes mechanical properties of the cartilage, resulting in loss of protective and weight-bearing functions.

Chondrocytes are the only cellular component of articular cartilage, and are responsible for regulating the homeostasis of cartilage and the turnover of ECM. Chondrocytes are derived from mesenchymal stem cells (MSCs) in the bone marrow through a series of differentiation process (Chen *et al.*, 2021). Physiologically, chondrocytes in hyaline cartilages could produce various types of collagens, including collagen type II, IX, and XI, of which more than 90% are type II collagens (Charlier *et al.*, 2019; Eyre, 2002). Proteoglycans are another major product of articular chondrocytes to form the cartilage matrix, and aggrecans are the most abundant type of proteoglycans by weight in the hyaline cartilage (Roughley *et al.*, 1994). Thus, type II collagen and the aggrecan are also recognized as the specific markers of articular chondrocytes (Caron *et al.*, 2012; Chijimatsu *et al.*, 2019). However, during the progression of OA, chondrocytes would experience phenotype shift to more mature phenotypes with changes in synthetic activities (Charlier *et al.*, 2016). The hypertrophic change of articular chondrocytes is currently the most recorded phenotype (Ripmeester *et al.*, 2018; Singh *et al.*, 2019), while studies have confirmed that chondrocytes undergo various types of phenotypic changes in OA pathogenesis, including a dedifferentiated-like change (Aigner *et al.*, 2007; Charlier *et al.*, 2019).

The dedifferentiated-like phenotypic changes of chondrocytes have been observed within OA cartilage when the ECM stability and integrity are compromised, as an attempt to repair the damage (Pearle *et al.*, 2005; Zaucke *et al.*, 2001). Similarly, differentiation of

chondrocytes would happen after isolation from the cartilage and cultured in monolayers (Allen *et al.,* 2012; Lin *et al.,* 2008). Despite physiologically exhibiting a very low mitotic activity, chondrocytes can transition to an "active" state and proliferate rapidly in response to the stimulation of cartilage injury, which however, results in the production of non-hyaline cartilaginous ECM (Chen *et al.,* 2021; Pearle *et al.,* 2005). Dedifferentiated chondrocytes would produce less amount of aggrecans and type II collagen and initiate the synthesis of type I and III collagens (Charlier *et al.*, 2019), resulting in a fibrotic remodeling of articular cartilages in OA (Chan *et al.,* 2018; Deroyer *et al.*, 2019). Furthermore, a major transcription factor required for the expression of collagen type II alpha 1 (*COL2A1*) gene and cartilage formation, SRY-box transcription factor 9 (SOX9), have been found to be downregulated during the dedifferentiation of mouse chondrocytes (Bi *et al.,* 1999; Lefebvre *et al.,* 1997). This loss of the normal anabolic phenotype of chondrocytes leads to s regenerative property of articular cartilage, in which efforts on promoting the redifferentiation of dedifferentiated chondrocytes should provide new targets of interest for the development of OA treatment.

Given the degenerative nature of the OA, it is unlike to reverse the pathological process of the disease and repair the damaged joint structures with existing medical techniques, and surgical treatments such as total joint replacement, could only be considered as a salvation in the late-stage OA cases (Taruc-Uy *et al.,* 2013; Weinstein *et al.,* 2013; Yu *et al.,* 2015). Therefore, current treatment strategies for OA mainly could focus on medical management using physiological or pharmacological approaches to relief the pain and slow down the progression of OA, thereby improving the patients' quality of life and delaying the necessity for a surgical intervention (Ghouri *et al.,* 2019; Mobasheri, 2013; Mora *et al.,* 2018). Conventional pharmacological options for OA include paracetamol, opioids, nonsteroidal anti-inflammatory drugs (NSAIDs), and intra-articular drugs such as steroids and hyaluronic acid, which, however, could not attenuate the degradative changes in the joint and commonly associate with side effects (Ghouri *et al.,* 2019; Mobasheri, 2013; Weinstein *et al.,* 2013; Yu *et al.,* 2015). With the increasing understanding of the biomolecular mechanism of OA pathogenesis, disease modifying osteoarthritic drugs (DMOADs), a novel type of

pharmacological agents capable of reversing the progression of OA and the pathological damage of the joint, have been developed in the last decades (Anandacoomarasamy *et al.*, 2010; Ghouri *et al.*, 2019; Oo *et al.*, 2021; Oo *et al.*, 2022), including a semi-synthetic polysaccharide substance called pentosan polysulfate sodium (PPS) (Kumagai *et al.*, 2010). Although some of the DMOADs has been used in animals in certain parts of the world to manage the OA symptoms, wider use of these drugs is still restricted due to insufficient clinical and laboratorial information on the effects and mechanisms of actions of DMOADs (Ghouri *et al.*, 2019; Oo *et al.*, 2022). The unmet needs of disease-modifying drugs require further studies to reveal the molecular mechanisms involved in OA pathogenesis and the biomedical mechanisms of DMOADs.

Among the DMOADs, PPS is a mixture of structurally complex heterogenous sulfated polysaccharides derived from the wood of German beech. PPS is chemically semi-synthetic through a non-selective and exhaustive sulfate replacement of the hydroxyl groups on the second and third positions of a β-(1→4)-linked liner glucuronoxylan hemicellulose, giving PPS an average molecular weight of 4,000–6,000 Da molecular weight and a 2.0 sulfate level on each monosaccharide (Alekseeva *et al.*, 2020; Lin *et al.*, 2019). Due to the structural similarities, PPS is considered as a low molecular weight mimic of glycosaminoglycans, or more specifically, a heparin mimic (Ghosh, 1999; Lin *et al.*, 2019). In the body, glycosaminoglycans exist as free form of glycans or participant in forming surface receptors and ligands, and regulate a wide range of biological and cytological reactions, e.g., cell-cell adhesions and communications, cell proliferations, binding to growth factors or cytokines, or enzymatic reactions (Linhardt *et al.*, 2004; Mizumoto *et al.*, 2015; Xu *et al.*, 2014). Besides the physiological and pathological effects, glycosaminoglycans (e.g., heparin and chondroitin sulfate) has been used for many pharmaceutical purposes. Glycosaminoglycans mainly exert the biological activities through the interaction with proteins, which predominately depends on the ionic interactions between the negatively charged residues (mainly sulfate groups) of glycosaminoglycans and the basic amino acid residues (i.e., arginine, histidine, and lysine) of proteins, together with a structural complementarity

between the molecules (Meneghetti *et al.*, 2015; Ori *et al.*, 2011; Thompson *et al.*, 1994). The average molecular weight of glycosaminoglycans is considered an important parameter for their biomedical applications (Palhares *et al.*, 2021; Wang *et al.*, 2012), and previous studies have shown that high and low molecular weight of the same type of glycosaminoglycans could exert diverse therapeutic properties (Haas, 2003; Yang *et al.*, 2012). In addition to the molecular weight difference, the negative charge density of glycosaminoglycans is also relates to the number of anionic groups, which change the interaction between glycosaminoglycans and proteins, resulting in diverse pharmacological effects (Asperti *et al.*, 2015; El Masri *et al.*, 2017; Meneghetti *et al.*, 2015). The various biomedical effects caused by structural diversity has led to a growing interest in the glycosaminoglycans. Especially for the heparin substances, pharmacological studies have tried to verify the relation between the effects and its molecular mass and sulfation degree and to improve the manufacturing processes and expand its application (Chen *et al.*, 2021; Palhares *et al.*, 2021). However, the structure-effect relationship of PPS is rarely mentioned.

The present study aimed to investigate the properties of PPS, a novel DMOAD, on the proliferative activity of dedifferentiated canine articular chondrocytes and its effects in promoting the redifferentiation and ECM production of dedifferentiated chondrocytes, as well as the underlying mechanism of these effects. This study looked into the relation between these phenotypic regulatory effects of PPS and its structure. For these purposes, this study was divided into two subsections: Firstly, the effects of PPS in regulating chondrocyte cell cycle and the related phenotypic change were assessed in a monolayer culture. Differences in the effects between PPS with four sulfate levels from non-sulfate (0%) to full sulfate (19%) were also evaluated in the first section. Secondly, the anabolic effects of different molecular weights PPS in canine chondrocytes were further evaluated using a high-density micro-mass culture model, and the molecular weight-related effects were discussed. Previous findings suggested that PPS could enhance the combination between a disintegrin and metalloproteinase with thrombospondin motifs 5 (ADAMTS5) and tissue inhibitor of metalloproteinases 3 (TIMP3) to inhibit the activity of ADAMTS5, and PPS with molecular

mass from 3,300 Da showed more than 100-fold higher affinity for ADAMTS5 and TIMP3 than 2,400 Da PPS (Troeberg *et al.*, 2012). Considering this information with the common molecular weight of PPS (4,000–6,000 Da), PPS with molecular weights of 1,500, 3,000, 5,000, and 7,000 Da were chosen in section 2.

The information from this study could contribute to deepen the understanding of chondrocyte physiology and provide potential therapeutic strategies of OA in animals in the future. The finding on structure-effect relation of PPS could be beneficial for understanding the mechanism of PPS as a DMOAD and may help to improve its therapeutic effects.

Chapter I.

Sulfate Level Relied Effects of Pentosan Polysulfate Sodium on Inhibition of Cell Proliferation and Promotion of Chondrogenesis in Canine Articular Chondrocytes by Targeting PI3K/Akt Pathway

1.1 Summary

Physiologically as a type of post-mitotic cells, articular chondrocytes experience a dedifferentiated phenotype change in the development of OA, with transient increases in metabolic and proliferative activities, which leads to a reduced production of ECM components to form a normal cartilage structure. The phenotypic instability of chondrocytes accelerates cartilage degeneration and results in a low regenerative capacity of cartilages. Intervention of these phenomenon could be helpful for understanding chondrocytes physiology provides new hints for OA treatment. PPS is a semi-synthetic highly sulfated polysaccharide based on backbones of glucuronoxylan hemicelluloses, which has been applied for OA medical management in animals. This study investigated the efficacy of non-sulfated glucuronoxylan (defined as 0% sulfate level PPS) and three sulfate levels PPS (5, 16, and 19% as full sulfate; by the weight of sulfur atom) on the proliferative activity and cell cycle progression in monolayer-cultured canine articular chondrocytes, and the effects of promoting a chondrogenic differentiation in the chondrocytes. After a cultivation for 72 hr, PPS with full sulfate level significantly suppressed the proliferation of canine chondrocytes through inhibiting the transition of cell cycle from the G1 phase to later phases at higher concentration, while lower sulfate levels PPS did not exert significant effects. The results of quantitative real-time polymerase chain reaction (qPCR) confirmed that compared with the non-PPS-treated group, fully sulfated PPS significantly reduced the gene expression levels of cyclin dependent kinase 4 (*CDK4*) and cyclin D1 (*CCND1*), the key regulators for the G1/S phase transition in chondrocytes, in a concentration-dependent manner. Although the expression level of *CDK6* gene was not significantly different in all treatment groups when compared with the control. Meanwhile, the chondrocytes exposure to fully sulfated PPS upregulated the expression levels *COL2A1* and *SOX9* genes and downregulated the type I collagen alpha 2 chain (*COL1A2*) gene expression level compared with the non-treated group, indicated the PPS promotes a chondrogenic redifferentiation of monolayer-cultured chondrocytes. Furthermore, the results of Western blotting showed that the protein production of phosphatidylinositol 3-kinase catalytic subunit alpha (p110α), and the

phosphorylation of protein kinase B (Akt) were significant inhibited by full sulfate PPS after a 72 hr incubation. Interestingly, such effects of PPS in the chondrocytes were mostly found with full sulfate PPS, whereas lower sulfate levels PPS only showed weaker effects or had no effect. This study demonstrated phenotype and proliferation-regulatory effects of PPS in dedifferentiated articular chondrocytes, and the inhibition of PI3K/Akt pathway might relate to these properties of PPS. These findings could provide information for the development of OA management. In addition, the study provides evidence that the full sulfate level maybe necessary for PPS to achieve its therapeutic effects in articular chondrocytes.

1.2 Introduction

Osteoarthritis is a multi-factorial joint disease characterized by progressively degenerative changes of multiple structures in the synovial joint, including synovial membranes, tendon and ligaments, subchondral bones, and articular cartilages (Kapoor, 2015; Neogi, 2013; Sanderson *et al.*, 2009). While studies in humans indicated high prevalence of OA in old population, a study has reported up to 6.6% dogs were clinically diagnosed with OA in the Britain (O'Neill *et al.*, 2014). With no doubt that OA is the most common type of joint diseases in the world, which leads to impaired joint functions and reduced quality of live, especially in senior populations (Kapoor, 2015; Neogi, 2013). Although many efforts have been made during the past decades, the underlying biomolecular mechanisms of OA pathogenic progression and the structural changes in the joints are still not fully explained (Glyn-Jones *et al.*, 2015).

The surface of joints is cover by a thin layer of hyaline cartilage that protects other tissues and provides flexibility of movements. Normal articular cartilages are devoid of blood vessels, nerves and lymphatic supply and consist of only one type of resident cell named chondrocyte, which is embedded in a collagen II-rich and proteoglycan-rich ECM produced by itself and plays a critical role in the maintenance of the ECM components (Akkiraju *et al.*, 2015; Fox *et al.*, 2009). Chondrocytes in hyaline cartilage physiologically maintain a post-mitotic state with very low a proliferative ability (Charlier *et al.*, 2016; Hwang *et al.*, 2007). However, they could experience a series of phenotypic shifts under pathological conditions. Despite previous studies mainly documented and discussed the hypertrophic phenotype in OA progression, recently, different degenerated chondrocyte phenotypes have identified and are considered to be associated with the pathological changes of cartilages (Charlier *et al.*, 2019; Sandell *et al.*, 2001). During the pathological development of OA, especially when the ECM surrounding the cells were lost, the post-mitotic chondrocytes rapidly upregulate their metabolic activity and proliferative activity and cluster to adjust the changes of the microenvironment, which has been suggested to associate with a dedifferentiate-like phenotypic change, leading to reduced production of normal ECM

components in the chondrocytes (Charlier *et al.*, 2016; Hall, 2019; Maldonado *et al.*, 2013). On the other hand, the dedifferentiated changes of chondrocytes characterized by the loss of normal phenotype, upregulated proliferation, increased metabolic activity, as well as an impaired ECM synthesis have also been observed when the chondrocytes were isolated from cartilages and *in-vitro* cultured in a monolayer condition (Lin *et al.*, 2008; García-Carvajal *et al.*, 2013). Thus, investigating the proliferation and phenotypic shifts of dedifferentiated chondrocytes and feasible pharmacological interventions for such changes using *in-vitro* monolayer-cultures could help to understand the disease progression of OA cartilage and provide a potential target for OA treatment.

The exist therapeutic interventions for OA are mainly palliative and are incapable of preventing the disease progression (Glyn-Jones *et al.*, 2015; Mora *et al.*, 2018; Sanderson *et al.*, 2009). For the reason, recent pharmacological studies have focused on the development of reagents called DMOADs that are able to modulate the progression of OA including the loss of cartilage.

Pentosan polysulfate sodium (PPS) is a semi-synthetic heparin-mimic polysaccharide derived from the European beech (Alekseeva *et al.*, 2020; Ghosh, 1999), which has been used for treatment of human interstitial cystitis in the past decades (Asperti *et al.*, 2020; Ophoven *et al.*, 2019). While clinical trials in humans or horses demonstrated that injection of PPS improved the clinical symptoms of osteoarthritic joints (Ghosh *et al.*, 2005; Kumagai *et al.*, 2010; Tsogbadrakh *et al.*, 2020), *in-vitro* studies found that PPS treatment could reduce the degradation of cartilage components, suppress mitogen-activated protein kinase signaling pathway and the expression of inducible-nitric oxide synthase stimulated by interleukin-1 beta in chondrocytes, and promoted chondrogenic properties in MSCs and chondrocytes (Akaraphutiporn *et al.*, 2020; Bwalya *et al.*, 2017a; Sunaga *et al.*, 2012). However, the underlying molecular mechanisms of PPS in regulating the proliferation and phenotypic change of chondrocytes are still not fully understood.

PPS is synthesized through an exhaustively non-selective chemical sulfonation on a

liner backbone of beechwood glucuronoxylan compounds, resulting in the sulfate level per monosaccharide of PPS reaches to approximately 2.0 (Alekseeva *et al.*, 2020; Ghosh, 1999; Lin *et al.*, 2019). Although the 4,000 to 6,000 Da average molecular weight is lower than naturally synthesized polysaccharide molecules, several studies have compared its properties with polysaccharides like heparin or sulfate heparinoid (Asperti *et al.*, 2020; Sanden *et al.*, 2017). The biological effects of polysaccharides mainly associate with an electrostatic interaction between the positive-charged basic amino acid residues on proteins and the negative-charged sulfur groups on polysaccharides (Meneghetti *et al.*, 2015; Rosenberg *et al.*, 1979), which the sulfate modification on the 2-O and 6-O positions of heparan sulfate and heparin could largely change their treatment effects (Asperti *et al.*, 2015; El Masri *et al.*, 2017; Meneghetti *et al.*, 2015). Nevertheless, the relation between the sulfate level of PPS and its treatment effects, particularly in chondrocytes, is still not explored.

This study aimed to look into the regulatory effects and its underlying mechanisms of PPS on the proliferative activities and the phenotypic changes of dedifferentiated canine chondrocytes using monolayer cultures; and to investigate how these effects various from PPS with different sulfate levels.

1.3 Material and Methods

1.3.1 Reagents

The materials and their sources in this study were as follow: type I collagenase, sodium hydrogen carbonate ($NaHCO_3$), penicillin G potassium, streptomycin sulphate, trypsin, and dimethyl sulfoxide (DMSO) were from Wako Pure Chemicals Industries (Osaka, Japan); Dulbecco's modified Eagle's medium (DMEM) was from GIBCO (Grand Island, NY, U.S.A.); Fetal bovine serum (FBS; Batch #: 87 BCBZ5443), radioimmunoprecipitation assay (RIPA) buffer, protease inhibitor cocktail, and bovine serum albumin (BSA) were from Sigma-Aldrich (St. Louis, MO, U.S.A.); 4-(2-hydroxyethyl)-1-piperazineethanesulfonic acid (HEPES), 3-(4,5-dimehylthiazolyl-2)2,5-diphenyltetrazolium bromide (MTT), ethylenediaminetetraacetic acid (EDTA), and Cell Cycle Assay Solution Deep Red were from Dojindo (Kumamoto, Japan); BAMBANKER® was from GC LYMPHOTEC (Tokyo, Japan); FITC Annexin V Apoptosis Detection Kit I was from BD Biosciences (Heidelberg, Germany); NucleoSpin RNA Purification Kit and Protein Quantification Assay Kit were from Macherey-Nagel (Dürren, Germany); M-MLV Reverse Transcriptase Kit and NuPAGE™ 4 to 12% Bis-Tris gel were from Invitrogen (Carlsbad, CA, U.S.A.); KAPA SYBR FAST qPCR Kit was from KAPA Biosystems (Woburn, MA, U.S.A.); Western Blot Ultra-Sensitive HRP Substrate was from Takara Bio Inc. (Otsu, Japan); the culture dishes and tubes were from Corning (Lowell, MA, U.S.A.).

Three types of PPS with sulfate level (weight by weight of sulfur atoms in the molecule) of 5 (OJ119A-07), 16 (OJ119A-08), and 19% (OJ119A-04; full sulfate level) and a glucuronoxylan without sulfate modification (OJ119A-06; indicates 0% sulfate level PPS) purchased from Oji Pharma Co. (Tokyo, Japan) were used in this study for the treatment. All these PPS were dissolved in PBS and adjusted to desired concentrations before using.

All antibodies for Western blotting in this study were purchased from Cell Signaling Technology (Danvers, MA, U.S.A.): antibodies against p110α (Cat. #4249), Akt (Cat. #9272), phosphor (p)-Akt (Cat. #9271), β-actin (Cat. #4970), and anti-rabbit IgG horseradish

peroxidase (HRP)-linked antibody (Cat. #7074).

1.3.2 Collection of canine chondrocytes

Canine articular chondrocytes collected from humeral heads of five dogs were used in the present experiment. Four samples were from four experimental beagles (3-4 years old) euthanized at the end of studies that did not affect the joints. One cartilage sample was from a mixed-breed dog (13 years old) received amputation due to the growth of tumor on the radius bone. collecting cartilage samples from clinic and experimental dogs was under the guidelines of the ethical approval obtained from Hokkaido University Institutional Animal Care and Use Committee (approval number: 12-0059). For the collection of chondrocytes, cartilage samples were dissected into small fragments, then transfer into a culture plate containing 0.3% type I collagenase in DMEM and incubated overnight at 37°C. After which, the supernatant was passed through a sterilized membrane filter to remove the cartilage fragments. The primary chondrocytes were then collected to a FALCON and centrifugated at 300×g for 5 min. After counting, the cells were plated into 100 mm polystyrene culture dishes with DMEM contained 10% FBS, 10 mM of HEPES, 25 mM of $NaHCO_3$, 100 Unit/mL of penicillin G potassium, and 73 Unit/mL streptomycin sulphate and culture at 37°C in 5% CO_2. When the primary chondrocytes reached to an 80-90% confluency, the cells were detached from the dishes with 0.05% of trypsin and 0.02% of EDTA prepared in phosphate buffered saline (PBS), collected, resuspended in BAMBANKER®, and cryopreserved in liquid nitrogen.

1.3.3 Chondrocytes culture and treatment

For this study, the chondrocytes were firstly expanded to the second passage, then plated in polystyrene culture plates at a cell density of 5.0×10^4 cells/cm^2 in DMEM with 10% FBS and incubated for 24 hr at 37°C for adherence. The cultured medium was then changed to fresh medium and the chondrocytes were exposure to PPS for 72 hr. Due to the different purposes, PPS concentration was different between the experiments.

1.3.4 Cell viability analysis

After seeded in 96-well plates and cultured for 24 hr, the culture medium was changed and the chondrocytes were treated with 0, 5, 10, 20, 40, 80, and 120 μg/mL of PPS with four sulfate levels for 72 hr, or incubated with 0 and 80 μg/mL of PPS for 24, 48, and 72 hr. The MTT assay was performed to evaluate the cell viability of canine chondrocytes using following protocol: after incubated with PPS, the chondrocytes were briefly washed by PBS, then incubated with 0.5 mg/mL MTT prepared in DMEM for 4 hr at 37 °C. After discharged the MTT solution, the formazan crystals formed by the cells were dissolved with DMSO and the absorbance at 570 nm was measured by a Multiskan FC microplate reader (Thermo Scientific, Vantaa, Finland), subsequently.

1.3.5 Cytotoxic analysis of PPS

The chondrocytes seeded in 6-well plates were incubated with 0 or 80 μg/mL different sulfate level PPS for 72 hr, detached with trypsin-EDTA solution, then collected into 1.5 mL polypropylene tubes. The chondrocytes were stained with FITC Annexin V Apoptosis Detection Kit I and the cell death of chondrocytes was checked on a FACS Verse flow cytometer (BD Biosciences) following manufacturer's protocol.

1.3.6 Cell cycle assay

Canine chondrocytes in 6-well plates were exposed to 0, 20, and 80 μg/mL of PPS with four sulfate levels for 72 hr, then collected into 1.5 mL polypropylene tubes. The chondrocytes were then stained with Cell Cycle Assay Solution Deep Red using the manufacturer's protocol, after which, the fluorescence was detected by flow cytometry. The quantitative analysis was performed using FlowJo (version 10.8.1; Treestar, Ashland, Oregon, U.S.A.) with a Watson Pragmatic model.

1.3.7 RNA isolation and qPCR analysis

After seeded in 6-well plates for 24 hr, the medium was changed and the chondrocytes were treated with various sulfate levels of PPS at 0, 5, 20, and 80 μg/mL for 72 hr. Total

RNA in the chondrocytes was isolated using NucleoSpin RNA Purification Kit according to the manufacturer's protocol. The concentration of the RNA was measured at absorbance of 260 nm on a spectrophotometry. One microgram of total RNA was reversely transcribed into cDNA with M-MLV Reverse Transcriptase Kit following the manufacturer's protocol. The gene expression level was checked by qPCR with a two-step method using KAPA SYBR FAST qPCR Kit. To confirm the efficiency of the primers between reactions, standard curve method was applied for all genes, and all reactions were validated by the exist of a single peak in a melt curve analysis. The relative expression levels of target genes were analyzed using a delta-delta Ct method and glyceraldehyde-3-phosphatedehydrogenase (*GAPDH*) gene was used as a reference gene. The primers for *CCND1*, *CDK4*, and *CDK6* genes were used to check the effect of PPS on the cell cycle progression. The phenotypic change of chondrocytes was evaluated with *COL1A2*, *COL2A1*, and *SOX9* gene expression levels. The sequence, domain, amplicon length and accession number of the primers are in Table 1.

1.3.8 Isolation of protein and Western blotting analysis

Monolayer-cultured canine chondrocytes were treated with PPS at 0, 5, 20, and 80 μg/mL for 72 hr. After which, the chondrocytes were wash three times with cold PBS and were lysed with cold RIPA buffer containing 1% protease inhibitor cocktail. The cell lysates were then collected in to 1.5 mL tubes and centrifugated at 13,000×g and 4°C for 20 min to remove the insoluble materials. Total protein concentrations were measured by a microplate reader at 570 nm with Protein Quantification Assay Kit. Totally, 4 μg protein of each sample was loaded on NuPAGE™ 4 to 12% Bis-Tris gels and separated by electrophoresis, then transferred to polyvinylidene difluoride (PVDF) membranes. The membranes were blocked with 3% BSA prepared in PBS supplemented with 0.1% Tween 20 (PBST) for 1 hr, following an overnight incubation with primary antibodies against p110α, Akt, p-Akt, and β-actin at 4°C. After washing trice with PBST, the membranes were incubated with HRP-linked secondary antibodies for 1 hr. The bands were developed by reaction with Western Blot Ultra-Sensitive HRP Substrate, then detected by an Image Quant LAS 4000 (GE Healthcare, Buckinghamshire, U.K.). The density of the target bands was calculated by

ImageJ (NIH, Bethesda, MD, U.S.A.). The productions of target proteins were normalized using β-actin protein levels, and the p-Akt protein level was normalized by the Akt.

1.3.9 Statistical analysis

Statistical analysis was performed using GraphPad Prism (version 9.2.0; GraphPad Software Inc., La Jolla, CA, U.S.A.). Quantitative results are shown as means with standard deviations (SDs). Statistical comparisons were firstly performed with analysis of variance (ANOVA). When a significance was found, Dunnett's test was used to compare between the PPS-treated groups and the control. $p < 0.05$ was considered statistically significant.

Table 1. The information of the primers for qPCR.

Gene symbol	Primer sequence	Domain	Amplicon (bp)	Accession
GAPDH	Forward: 5′-CTGAACGGGAAGCTCACTGG-3′	726–745	129	NM_001003142.2
	Reverse: 5′-CGATGCCTGCTTCACTACCT-3′	854–835		
CCND1	Forward: 5′-AGTGTGATGCGGACTGTCTC-3′	875–894	184	NM_001005757.1
	Reverse: 5′-GCGCACCCTCAAATGTTCAC-3′	1058–1039		
CDK4	Forward: 5′-TAGCTTGCGGCCTGTCTATG-3′	68–87	145	XM_038679138.1
	Reverse: 5′-CAGAGAAGACCCTCACTCGG-3′	212–193		
CDK6	Forward: 5′-AGCCAAACGTCCCTAGAAGC-3′	8915–8934	121	XM_038436151.1
	Reverse: 5′-GAGAGATGCCTGGTAGACGC-3′	9035–9016		
COL1A2	Forward: 5′-GTGGATACGCGGACTTTGTT-3′	150–169	164	NM_001003187.1
	Reverse: 5′-GGGATACCATCGTCACCATC-3′	313–294		
COL2A1	Forward: 5′-CACTGCCAACGTCCAGATGA-3′	4127–4146	215	NM_001006951.1
	Reverse: 5′-GTTTCGTGCAGCCATCCTTC-3′	4341–4322		
SOX9	Forward: 5′-GCCGAGGAGGCCACCGAACA-3′	565–583	179	NM_001002978.1
	Reverse: 5′-CCCGGCTGCACGTCGGTTTT-3′	743–724		

GAPDH = glyceraldehyde-3-phosphate dehydrogenase, *CCND1* = cyclin D1, *CDK4* = cyclin dependent kinase 4, *CDK6* = cyclin dependent kinase 6, *COL1A2* = type I collagen alpha 2 chain, *COL2A1* = type II collagen alpha 1 chain, *SOX9* = SRY-Box transcription factor 9.

1.4 Results

1.4.1 Fully sulfated PPS reduces chondrocyte viability in MTT assay

The MTT assay results showed a concentration-dependent effect of full sulfate level PPS on the cell viability of canine chondrocytes (Figure 1A). Chondrocyte cell viability was reduced after incubated with full sulfate PPS for 72 hr, with significant differences observed at 40 ($p = 0.001$), 80 ($p < 0.001$), and 120 ($p < 0.001$) μg/mL, respectively compared with the control. Beside in the full sulfate group, a reduced trend of cell viability was found in 16% PPS group at high concentrations. However, a significant difference was found only at 120 μg/mL ($p = 0.006$). The growth curves indicated chondrocyte viability increased slower than other groups when incubated with 80 μg/mL of full sulfate level PPS (Figure 1B). Significant reduction was observed in full sulfate groups at 48 ($p = 0.024$) and 72 ($p < 0.001$) hr when compared with the control. Significant effect on chondrocyte viability was not found in 0 and 5% PPS-treated groups at any concentrations or time points.

1.4.2 Change in sulfate level has no influence on cytotoxicity of PPS

The results of flow cytometry with annexin V and PI double-staining distributed the chondrocytes into live group and non-live groups (including necrotic cells, early apoptotic cells and late apoptotic cells). After incubated with a high concentration of PPS for 72 hr, the distribution of chondrocytes in the four areas was same between the groups (Figure 2A). The percentage of live cells in PPS-treated groups (0%: 96.17 ± 1.92; 5%: 96.75 ± 1.62; 16%: 96.87 ± 1.60; full: 96.25 ± 1.28) was not significantly different from those in the control group (96.18 ± 1.85), respectively (Figure 2B).

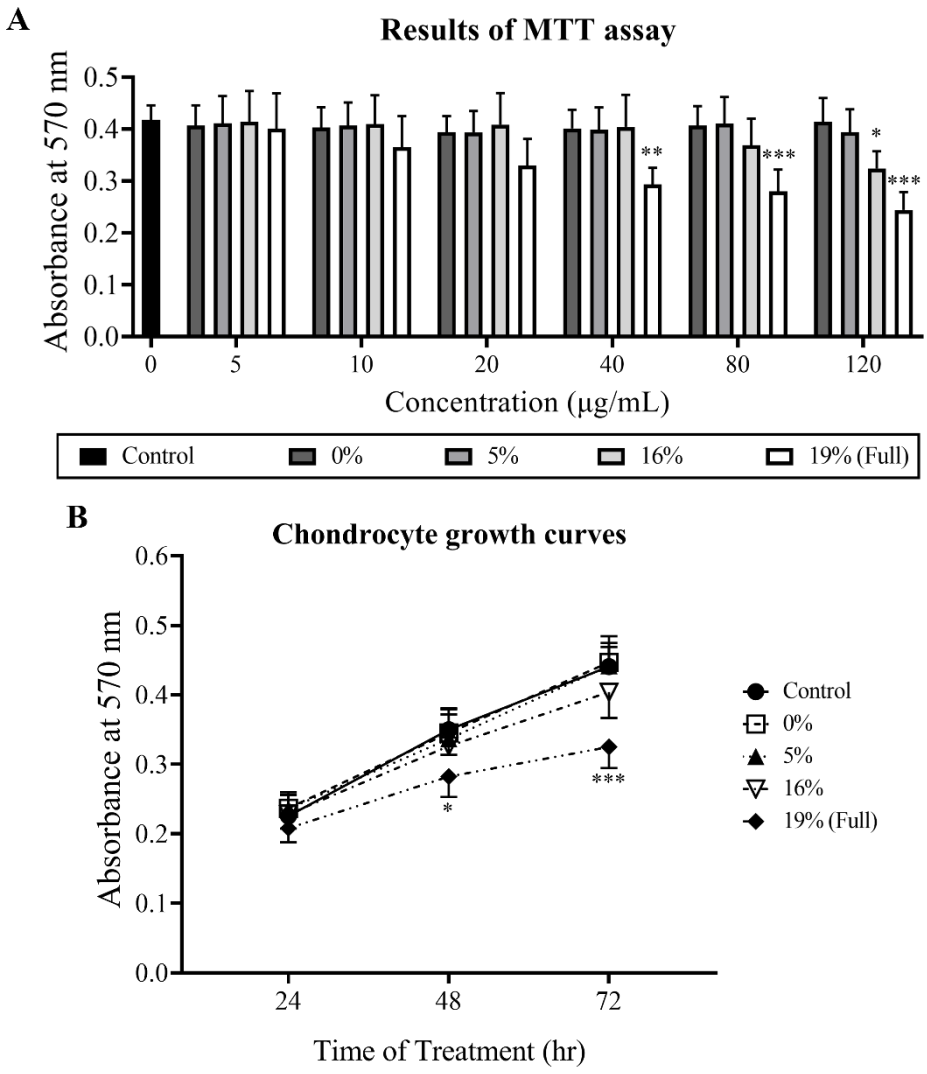

Figure 1. Full sulfate level PPS reduced chondrocyte viability.

The cell viability of monolayer-cultured canine chondrocytes was determined by MTT colorimetric assay at 570 nm. Chondrocytes were seeded in 96-well plates for 24 hr, (A) then treated with 0, 5, 10, 20, 40, 80, and 120 μg/mL of PPS (sulfate level: 0, 5, 16, and 19% as full sulfate) for 72 hr, (B) or treated with 0 and 80 μg/mL of PPS for 24, 48, and 72 hr. (A) Full sulfate level PPS significantly reduced the cell viability of chondrocytes at 72 hr, while other sulfate levels showed weakened or no effects. (B) Chondrocyte viability increased more slowly in full sulfate groups compared with the control. Data represent the means ± SDs (*$p < 0.05$, **$p < 0.01$, and ***$p < 0.001$).

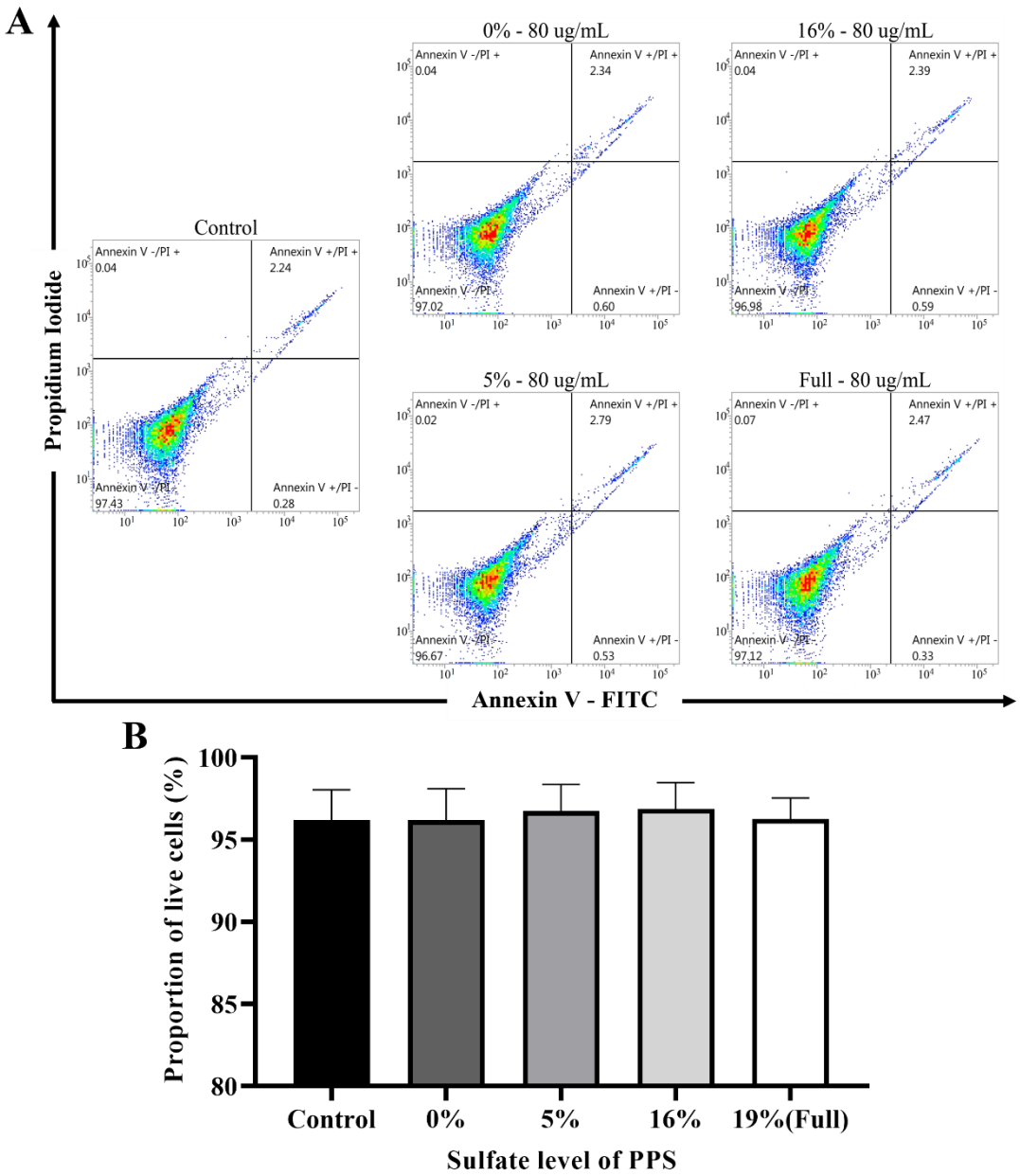

Figure 2. PPS with different sulfate levels showed same cytotoxic effects on chondrocytes.

Chondrocytes apoptosis was evaluated by flow cytometry with annexin V and PI staining. After 24 hr incubation, the chondrocytes were exposed to four sulfate levels of PPS (0, 5, 16, and 19% as full sulfate) for 72 hr. (A) Cells combined with annexin V-FITC and PI (Upper left: necrotic cells; upper right: late apoptotic cells; lower left: live cells; and lower right: early apoptotic cells). (B) The percentage of live cells. No significant difference was found between the treatment groups and the control. Data represent the means ± SDs.

1.4.3 Full sulfate level of PPS inhibits canine chondrocytes entering the subsequent phases of cell cycle from the G1 phase

After 72 hr exposure to PPS, the chondrocytes distributed in the G1, S, and G2 phase of the cell cycle were detected by flow cytometry according to the amount of in the cells (Figure 3). Compared with the non-treated group, the percentage of chondrocytes distributed in the G1 phase was significantly increased after incubated with full sulfate PPS at 80 μg/mL (p = 0.002). Meanwhile, the proportion of chondrocytes in the S (p > 0.05) and G2 (p = 0.037) phases in the full sulfate group was reduced (Table 2). No statistical significance was found between the control group and other PPS-treated groups. These results indicated that the chondrocytes proliferation was inhibited with 80 μg/mL of full sulfate level PPS treatment.

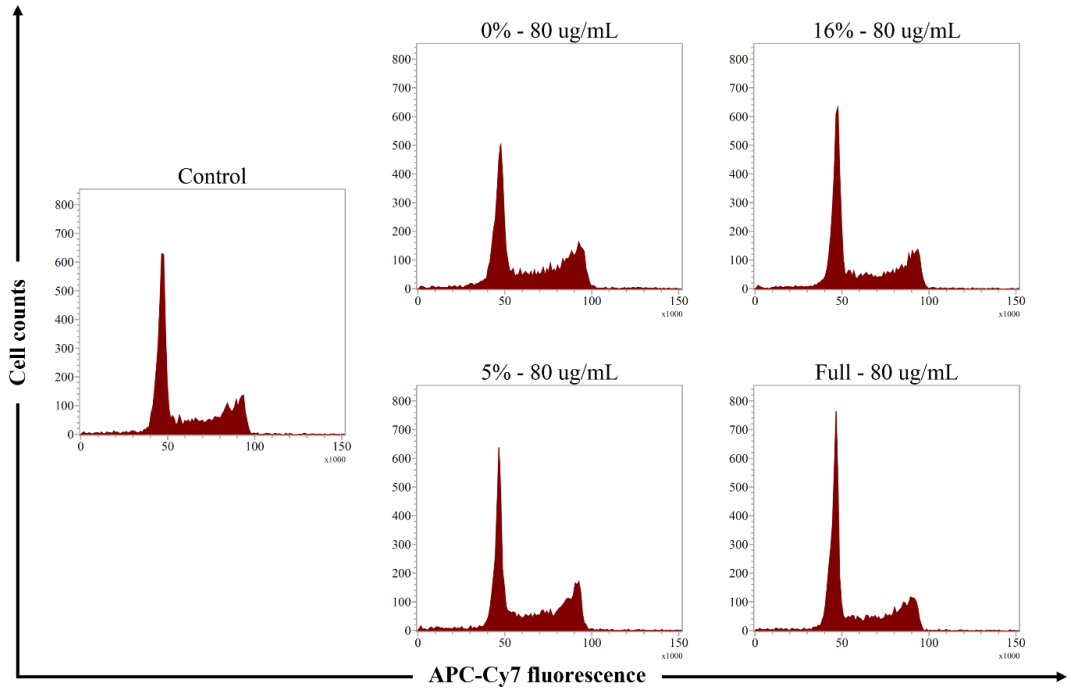

Figure 3. Cell cycle distribution of chondrocytes with nuclear DNA staining.

Chondrocytes were cultured for 24 hr, then received the treatment with 0, 20, and 80 μg/mL of various sulfate levels of PPS (0, 5, 16, and 19% as full sulfate) for 72 hr. Cell cycle analysis was performed on by flow cytometry with cell cycle assay solution staining. The histograms showed the distribution of chondrocytes in the control and 80 μg/mL PPS-treated groups.

Table 2. Quantitative results of chondrocyte distribution in the G1, S and G2 phase.

Phase	Control	0%	5%	16%	19% (Full)
	0	20 μg/mL			
G1 (%)	40.00 ± 2.87	38.90 ± 2.13	37.68 ± 2.68	39.68 ± 3.33	43.20 ± 2.27
S (%)	38.41 ± 2.13	38.76 ± 3.60	39.96 ± 3.16	37.73 ± 3.52	32.88 ± 2.71
G2 (%)	21.59 ± 2.28	22.34 ± 1.87	22.35 ± 2.56	22.41 ± 1.91	23.92 ± 2.72
		80 μg/mL			
G1 (%)		35.61 ± 4.33	35.80 ± 3.49	39.12 ± 4.20	48.14 ± 2.27[(a)]
S (%)		41.42 ± 4.61	41.65 ± 2.69	39.74 ± 3.90	34.38 ± 1.11
G2 (%)		22.97 ± 2.44	22.55 ± 2.56	21.13 ± 2.04	17.48 ± 1.25[(b)]

Full sulfate level PPS significantly increased the percentage of chondrocytes in G1 phase while reduced the percentage of cells in S and G2 phase. Data present the means ± SDs. (a) $p = 0.002$ and (b) $p = 0.037$.

1.4.4 Fully sulfated PPS decreases the gene expression of cell cycle regulators for G1/S transition and upregulates the expression of chondrogenic phenotype related genes

After 72 hr treated with PPS, the expression levels of *CCND1*, *CDK4*, and *CDK6*, the regulators for G1/S transition of chondrocyte cell cycle, was evaluated by qPCR. The mRNA levels of *CCND1* and *CDK4* were concentration-dependently reduced with full sulfate level PPS treatment, which significant differences of *CCND1* ($p = 0.003$) and *CDK4* ($p = 0.002$) levels were found at 80 μg/mL, compared with the control (Figure 4A and B). The gene expression of *CDK6* in PPS-treated groups was not significantly different from the non-treated group at all concentrations (Figure 4C). The expression levels of phenotypic gene markers, *COL1A2*, *COL2A1*, and *SOX9*, was also checked in the chondrocytes. The mRNA level of *COL1A2* was significantly downregulated in full sulfate level PPS group at 5 μg/mL ($p = 0.029$) when compared with the non-treated group (Figure 4D). However, significant difference cannot be found at higher concentrations. In contrast, the qPCR results indicated significant increases of *COL2A1* expression levels in the chondrocytes after incubated with full sulfate PPS at 20 ($p < 0.001$) and 80 ($p < 0.001$) μg/mL, respectively compared with the control group (Figure 4E). The *SOX9* gene expression was also upregulated with full sulfate level PPS-treatment, and a significant different was found at 80 μg/mL (Figure 4F).

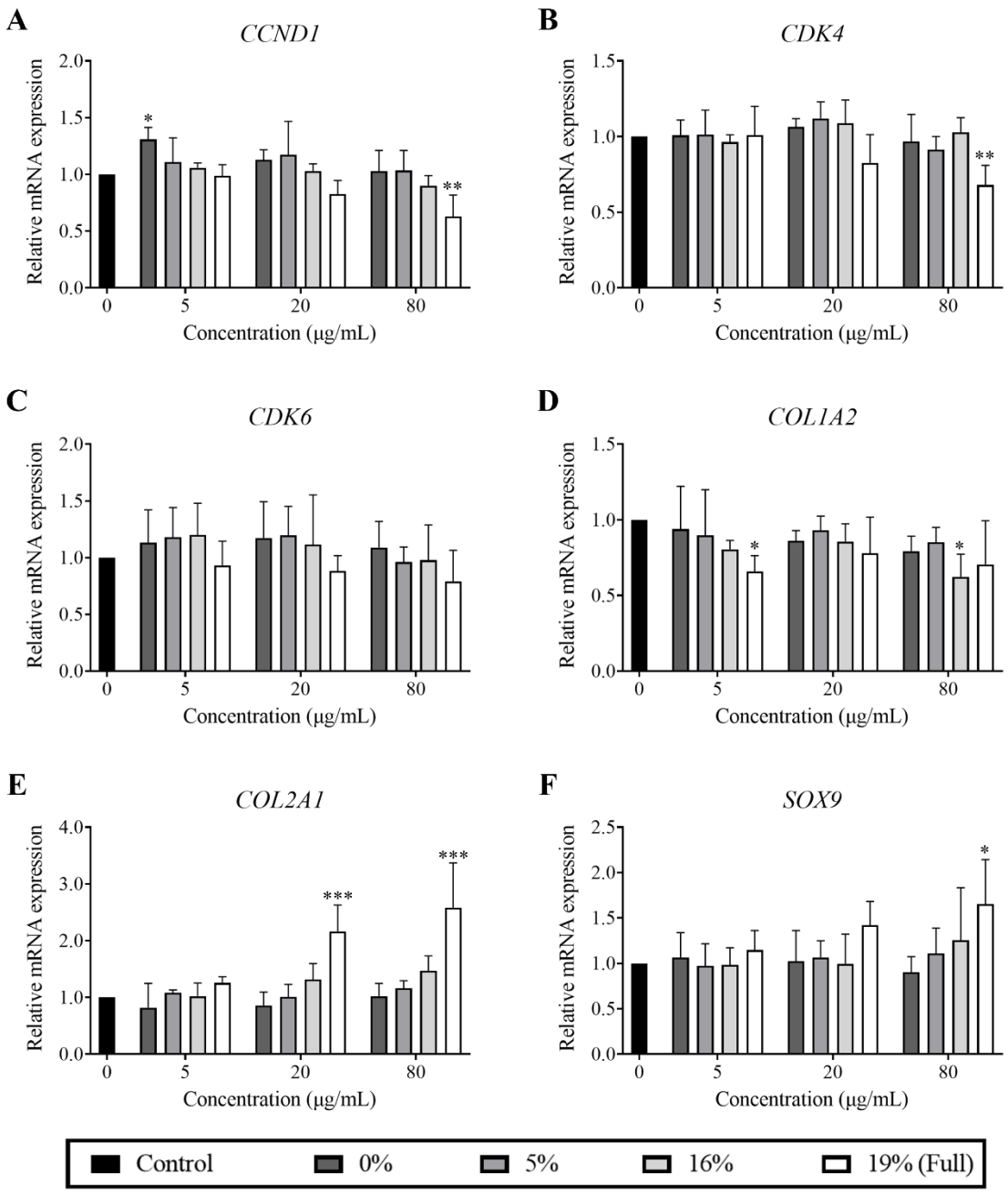

Figure 4. Fully sulfated PPS reduced *CCND1* and *CDK4* mRNA levels, while upregulated *COL2A1* and *SOX9* gene expression.

After incubated with different sulfate levels of PPS (0, 5, 16, and 19% as full sulfate) for 72 hr, mRNA levels of canine chondrocytes were evaluated by qPCR. Relative gene expression levels of (A) *CCND1* and (B) *CDK4* were significantly downregulated with full sulfate PPS at 80 μg/mL, while the expression levels of (E) *COL2A1* and (F) *SOX9* were upregulated in a concentration-dependent manner. Data represent the means ± SDs (*$p < 0.05$, **$p < 0.01$, and ***$p < 0.001$).

1.4.5 PI3K/Akt signaling pathway is suppressed by PPS with full sulfate level

The protein production of p110α and the phosphorylation of Akt were evaluate in canine chondrocytes after treated with different sulfate levels of PPS (Figure 5A). Significant reductions of p110α protein production were observed in the chondrocytes incubated with 20 (p = 0.044) and 80 (p = 0.001) μg/mL of full sulfate PPS for 72 hr, compared to the control respectively (Figure 5B). Consistent with p110α protein production, Akt phosphorylation in the chondrocytes was significantly inhibited with full sulfate PPS at 5 (p = 0.026), 20 (p = 0.029), and 80 (p = 0.003) μg/mL (Figure 5C). However, no more significant difference in p110α production or Akt phosphorylation can be observed between lower sulfate level groups and the control, except a significant reduced p110α protein production in 5% PPS group at 80 μg/mL (p = 0.040; Figure 5B).

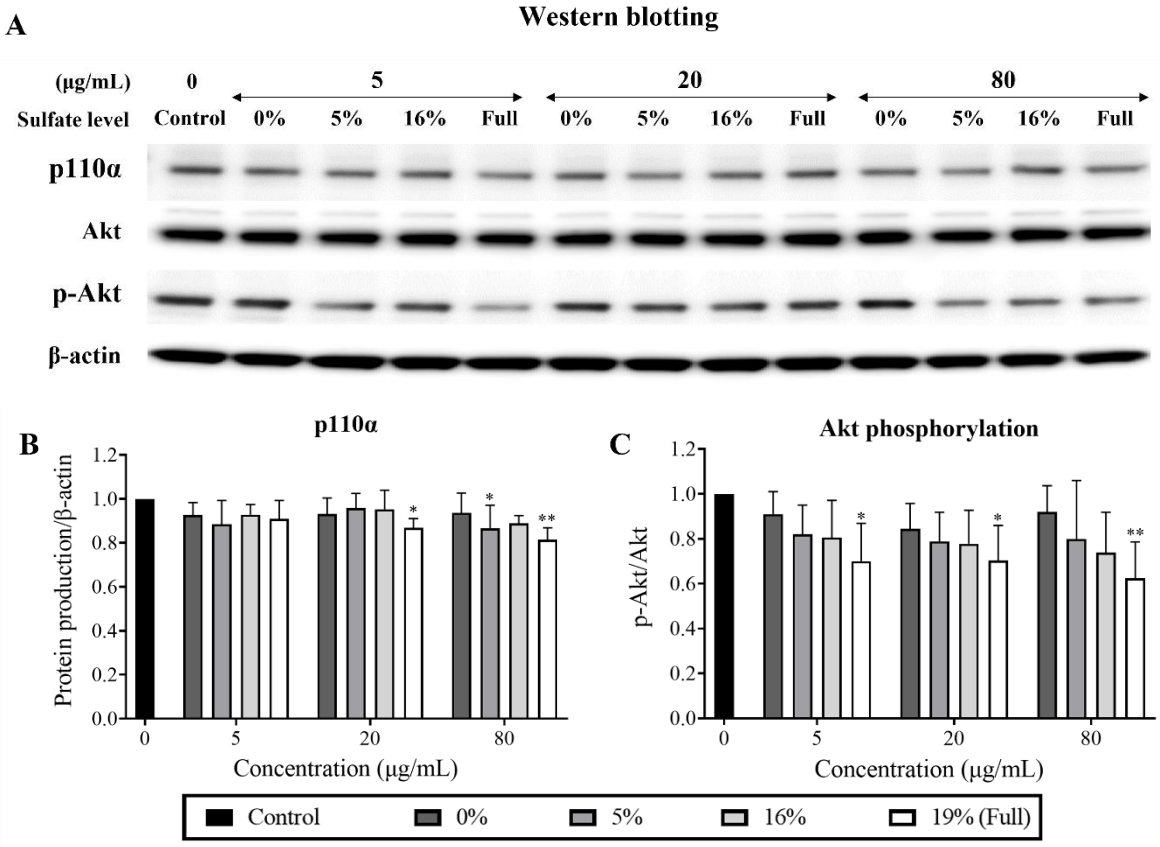

Figure 5. The protein production of p110α and phosphorylation of Akt were suppressed by PPS with full sulfate level.

Chondrocytes were cultured with four sulfate levels of PPS (0, 5, 16, and 19% as full sulfate) at 5, 20, and 80 μg/mL for 72 hr. (A) The protein production of p110α, Akt and p-Akt in canine chondrocytes were determined by Western blotting. (B) p110α protein production was significantly reduced with full sulfate PPS treatment at 20 and 80 μg/mL compared with the control group. (C) The phosphorylation of Akt was concentration-dependently inhibited after incubated with full sulfate PPS. Data are the means ± SDs (*$p < 0.05$ and **$p < 0.01$).

1.5 Discussion

In the present study, the effects of PPS on inhibiting the proliferation and promoting the redifferentiation of chondrocytes and the underlying mechanisms of these effects were investigated in a monolayer culture model. As post-mitotic cells, articular chondrocytes exhibit low a proliferative activity under physiological condition (Charlier *et al.*, 2016; Hwang *et al.*, 2007). However, when the microenvironment is disturbed, chondrocytes could undergo a dedifferentiated phenotype change characterized by upregulated proliferative activity and reduced ECM production, which has been observed during the disease progression of OA or in chondrocyte *in-vitro* monolayer cultures (Charlier *et al.*, 2016; Hall, 2019; Lin *et al.*, 2008). Intervention of the dedifferentiation-related changes of chondrocytes could deepen the understanding of OA pathogenesis and provide hints for the development of OA medical management.

A significant reduction of chondrocyte viability was detected by MTT assay in full sulfate PPS group when the concentration was higher than 40 μg/mL, while flow cytometry analysis showed that the percentage of dead cell in all PPS-treated groups was no raised even at 80 μg/mL. MTT assay was performed to check the potential cytotoxicity of PPS and provide a reference of concentration for the subsequent experiments. Since MTT assay measures the chromogenic formazan crystals produced by live cells, previous studies have shown that the results could be influenced by both proliferation and cell death, suggesting that the results of MTT assay should be combined with other methods to interpret cytotoxic effects. (Kumar *et al.*, 2018; Sylvester, 2011). For the reason, the cell death of chondrocytes was determined by flow cytometry with annexin V-FITC and PI staining. This study demonstrated that PPS with sulfate levels from 0 to 19% (full sulfate) could be safely used to treat chondrocytes, which was consistent with previous findings (Akaraphutiporn *et al.*, 2020; Ghosh, 1999; Ghosh *et al.*, 2010). On the other hand, the growth curves showed that the increase rate of chondrocyte viability in 19% PPS-treated group was significantly slower than that in the control group, which suggested the reduced cell viability with full sulfate level PPS treatment should be associated with the inhibition of cell proliferation.

Full sulfate PPS treatment increased the proportion of chondrocytes in the G1 phase of cell cycle and reduced the number of chondrocytes entering S and G2 phase, while the significant effects were observed only at 80 μg/mL. During the proliferation of eukaryotic cells, cell cycle is divided into G1, S, G2, and M phase, which could be identified according to the different nucleus DNA contents (Beier *et al.*, 1999; Nurse, 2000). To evaluate the inhibitory effects of PPS with various sulfate level on the proliferative activity of chondrocytes, the cell cycle progression of was analyzed with DNA stain. Unlike a previous study demonstrated that high-concentration PPS treatment increased the percentage of chondrocytes in the G1 phase only at 24 and 48 hr but not at 72 hr (Akaraphutiporn *et al.*, 2020), the present study showed that the increased proportion of chondrocytes in the G1 phase could be observed at 72 hr. The proliferative potential of chondrocytes at a seeding density of 5.0×10^4 cells/cm^2 should remain high at the ending point in this study, since previous studies have represented that with similar seeding densities, the number of chondrocytes continuously increased in the first week of culture (Akaraphutiporn *et al.*, 2020; Watt, 1988). One possible explanation would be that the chondrocyte specimens in the previous study were collected from the joints with clinical signs, which could result in an early cluster formation in the culture and activated the contact inhibition of chondrocytes (Gérard *et al.*, 2014; Hall, 2019; Maldonado *et al.*, 2013). Overall, the findings in the present study were consistent with previous studies that full sulfate PPS inhibits the progression of cell cycle from the G1 phase to later phases, there by inhibiting the proliferative activity of chondrocytes.

The results of qPCR showed that chondrocytes treated with 80 μg/mL full sulfate PPS significantly downregulated the expression levels of *CDK4* and *CCND1* genes. A reduced trend of *CDK6* mRNA level was also found in full sulfate PPS group, while no significant difference between the PPS-treated groups and the control was found. In mammalian cells, the cell cycle was regulated by several checkpoints. In the G1 phase, CDK4 and 6 combine with cyclin D to form a catalytic complex, which control the G1/S phase transition by phosphorylating the retinoblastoma protein (Beier *et al.*, 1999; Berridge, 2014; Qu *et al.*,

2003). To explore how PPS involves into cell cycle regulation in chondrocytes, the expression levels of *CDK4*, *CDK6*, and *CCND1* genes were then evaluated. In agreement with the increased percentage of chondrocytes in G1 phase and the reduced percentage in S and G2 phase, reduce *CDK4 CCND1* genes expression was confirmed. On the other hand, previous studies have reported that the proliferation of fibroblasts and retinal pigment epithelium cells was promoted by activating the PI3K/Akt signaling pathway (Dai *et al.*, 2019; Parrales *et al.*, 2011). Similarly, the proliferative activity of chondrocytes was found to regulated by the PI3K/Akt pathway (Huang *et al.*, 2011; Liang *et al.*, 2018; Tao *et al.*, 2020). In the present study, the results of Western blotting revealed that p110α protein production and Akt phosphorylation in canine chondrocytes were inhibited with full sulfate PPS treatment at higher concentrations. Based on these results, it seems reasonable to consider that PPS suppresses the proliferation of chondrocytes by targeting the PI3K/Akt signaling pathway and the expression of *CDK4* and *CCND1*.

The expression levels of *COL2A1* and *SOX9* gene were increased in monolayer-cultured chondrocytes after exposure to full sulfate PPS for 72 hr, which were negatively corresponded with the mRNA levels of *CDK4/6* and *CCND1*. In contrast, *COL1A2* mRNA level was downregulated after treated with full sulfate PPS, while a significant reduction was found at 5 μg/mL. *COL2A* is a specific marker for hyaline cartilage, and *SOX9* is an essential transcription factor for ECM formation in chondrocytes. (Gelse *et al.*, 2012; Mao *et al.*, 2018; Ripmeester *et al.*, 2018). Upregulated expression of these genes indicated that PPS stimulated the redifferentiation of the chondrocytes. The finding of the relation between cell cycle regulators and phenotype markers was consistent with previous studies, which indicated that the expression of collagen II and SOX9 was negatively correlated with the level of CDK6 and cyclin D1 in *in-vitro* cultured chondrocytes (Akaraphutiporn *et al.*, 2020; Hwang *et al.*, 2007; Parreno *et al.*, 2017). The PI3K/Akt pathway plays an important role in regulating chondrocyte phenotype and ECM production. Inhibition of the PI3K/Akt pathway has been shown to attenuate the hypertrophic and fibroblastic differentiation of human chondrocytes and increase the production of type II collagen, aggrecan, and SOX9 in the

chondrocytes at gene and protein levels (Liu *et al.*, 2020). Nevertheless, other studies have reported that collagen II production in human and rabbit chondrocytes was increased via Akt pathway (Eo *et al.*, 2014; Hwang *et al.*, 2020). Although its function in the anabolic activity of chondrocytes remains puzzling, the reduced p110a production and inhibited Akt phosphorylation in the present study indicated that PPS may suppress the proliferation and promote redifferentiation of monolayer-cultured chondrocytes both though inhibition of PI3K/Akt signaling pathway.

This study carries a major purpose to investigate the relationship between the sulfate level of PPS and its beneficial effects in chondrocytes. During the semi-synthetic process, the 2-O and 3-O hydroxyl groups on the glucuronoxylan backbone of PPS are non-selectively and exhaustively sulfated (Alekseeva *et al.*, 2020; Lin *et al.*, 2019). This highly sulfated structure based on a hemicellulose makes PPS to be considered as a mimic of glycosaminoglycan compounds (Ghosh, 1999; Lin *et al.*, 2019). Treatment with glycosaminoglycans, including heparan sulfate, heparin, and dermatan sulfate, has been shown to stimulate chondrogenesis in MSCs *in-vitro*, and the molecular size, charge, and chemical structure of the glycosaminoglycans could largely affect these activities (Park *et al.*, 2008; San Antonio *et al.*, 1987). Furthermore, a more recent study reported that GY785 DRS, an over sulfated isoform of the polysaccharide GY785 DR, showed 100-fold higher affinity than GY785 DR in binding to transforming growth factor beta 1, and exerted stronger effects in stimulating the chondrogenic differentiation and cartilage-like ECM production of human MSCs (Merceron *et al.*, 2012). In the present study, the effects of glucuronoxylan (0%) and PPS with sulfate levels of 5, 16, and 19% (full sulfate) in chondrocytes were investigated. Notably, only full sulfate PPS showed significant effects in inhibiting the proliferation, promoting the redifferentiation, and suppressing the activation PI3K/Akt pathway in monolayer-cultured chondrocytes. PPS with 16% sulfate level exerted insignificant effects, and the effects of 0 and 5% sulfate PPS in chondrocytes were not detectable in this study. These data suggested that to achieve the treatment effects of PPS in chondrocytes, full sulfate level with sulfur groups on the 2-O and 3-O positions of PPS might be essential.

In conclusion, the present study confirmed that PPS inhibited the proliferation of monolayer-cultured canine chondrocytes via *CDK4/6* and *CCND1* expression levels, in turn to suppress the G1/S transition of the cell cycle. Meanwhile, PPS promoted the redifferentiation of chondrocytes, confirmed by the upregulated *COL2A1* and *SOX9* gene expression. Furthermore, the regulation of differentiation in chondrocytes by PPS might be achieved by targeting PI3K/Akt signaling pathway. Since increased proliferative activity with reduced production of ECM compounds in chondrocytes is observed in the early stage of OA development, this study suggested that PPS could be beneficial for OA treatment by suppressing the activated proliferative state and restoring the lost normal phenotype of dedifferentiated chondrocytes, in turn to retore the micro-environment in the articular cartilages. Another novel finding is the significant effects on either the proliferation or the phenotype changes of chondrocytes were only observed in the full sulfate PPS group, which suggested that the sulfate level of PPS could be a key factor for its biological effects, and an exhaustive sulfonation seems to be necessary for PPS to exert therapeutic effects in articular chondrocytes.

Chapter II.

Pentosan Polysulfate Sodium Promotes Redifferentiation to the Original Phenotype in Micromass-Cultured Canine Articular Chondrocytes and Exerts Molecular Weight-Dependent Effects

2.1 Summary

Differentiation of articular chondrocytes occurs during the pathogenesis of OA, which reduces the ability of chondrocytes to produce normal ECM components, and eventually leads to the loss of normal biomechanical function of articular cartilage. PPS is a semi-synthetic DMOAD derived from European beech wood, which has been applied as a therapeutic treatment of OA in animals. The present study investigated the phenotype regulatory efficacy of PPS with four molecular weights (1,500, 3,000, 5,000, and 7,000 Da) in dedifferentiated canine chondrocytes and the effects of these PPS in promoting chondrocyte ECM synthesis. Monolayer-cultured canine chondrocytes were firstly exposure to high concentration of PPS for 72 hr to evaluate the potential cytotoxic effects of PPS The flow cytometry and MTT assay results showed that PPS with all the molecular weight was safe to chondrocytes. In the next, the effects of PPS on the phenotypic change and ECM production of chondrocytes were determined in a 12-day chondrocyte micro-mass culture model. After incubated with different molecular weight PPS at concentrations of 0, 5, 10, and 40 μg/mL, the results of qPCR showed that PPS promotes a redifferentiation of the chondrocytes in a concentration-dependent and molecular weight-dependent manner, which was evidenced by significantly upregulated *COL2A1*, *ACAN*, and *SOX9* mRNA expression levels and collagen II and SOX9 protein productions in higher molecular weights PPS-treated groups compared with the control. However, mRNA level of *COL1A2* in the chondrocytes was simultaneously increased in 7,000 Da PPS-treated group. In addition, PPS molecular weight-dependently inhibited the phosphorylation of Akt in micro-mass-cultured chondrocytes and a significant reduction was found in 7,000 Da PPS group at 40 μg/mL. The results of Alcian blue staining of the micro-mass cultures evidenced an enhanced proteoglycans deposition in the ECM of the chondrocytes after a 72 hr treatment with PPS, in which stronger staining was observed in 5,000 and 7,000 Da PPS-treated groups. This study clearly indicates that PPS promoted the redifferentiation of dedifferentiated canine chondrocytes not just in a monolayer culture, but in a more *in-vivo*-like environment in micro-mass culture, and increasing the molecular weight of PPS could enhance these

phenotype-regulatory effects. The finding of this study may provide a potential target for OA treatment and could help optimize the therapeutic effects of PPS.

2.2 Introduction

Osteoarthritis affects multiple joint structures and is considered as the most common type of canine joint disease leads to loss of joint function, which approximately 20% of dogs presenting with clinical symptoms (Goldring, 2012; Kuyinu *et al.*, 2016; Shah *et al.*, 2018). Articular hyaline cartilage covers the joint surface and is rich in type II collagen as well as proteoglycan components, which combines a large amount of water that support the tensile force and compressive strength put on the joint surface to protect the subchondral bone (Medvedeva *et al.*, 2018). Despite lacking blood supply, lymphatic system, and nerves, articular cartilage is composed of only one type of cell called chondrocyte surrounded by ECM formed by itself (Archer *et al.*, 2003; Goldring, 2012). As the only cell component within the cartilage, chondrocytes are responsible for renewing the ECM composition and maintaining the cartilage homeostasis (Ripmeester *et al.*, 2018; Fox *et al.*, 2009). However, under an OA condition, chondrocytes have been found to undergo a dedifferentiated process, characterized by accelerated cell proliferation, increased secretion of matrix-degrading enzymes and less productive in essential ECM components for cartilage (Goldring *et al.*, 2009), which rises a great challenge for maintaining a functional structure of cartilage and repairing the cartilage defect caused by the disease progression. Although more work needs to be done for investigating the mechanism of these dedifferentiation-related changes of OA chondrocytes, studies on the intervention of these events could provide promising pharmacological treatment for OA.

The pathological progress of OA is irreversible with current therapies. Medications developed for therapeutic interventions of OA can be recognized as releasing the clinical symptoms or as controlling the progression of the disease (Henrotin *et al.*, 2005; Medvedeva *et al.*, 2018). PPS is a heparin-like semi-synthetic compound derived from European beech-wood hemicellulose (Kumagai *et al.*, 2010). The structure of PPS contains the backbone of repeating (1-4)-linked-β-D-xylano-pyranoses units with sulfate esterification (Alekseeva *et al.*, 2020). The molecular weight of its sodium salt is varied in different products, which most of them ranged from 4,000 to 6,000 Da, with an average of 5,700 Da (Kumagai *et al.*,

2010). Although PPS has been used as antithrombotic-and-antilipidemic drugs for long time in Europe (Ghosh, 1999), its effects on improving the synovial fluid quality, inhibiting cartilage degeneration, and promoting the chondrogenic differentiation and the ECM production of MSCs have been demonstrated (Akaraphutiporn *et al.*, 2020; Bwalya *et al.*, 2017a; Bwalya *et al.*, 2017b; McIlwraith *et al.*, 2012; Wu *et al.*, 2017). However, the mechanism of PPS on cartilages and chondrocytes is not fully understand.

PPS shares a similar structure with naturally sulfated glycosaminoglycans like heparin or heparin sulfate (Alekseeva *et al.*, 2020). For the reason, several studies therefore have described the resemblance in anti-coagulant or anti-inflammatory effects between heparin and PPS (Esquivel *et al.*, 1982; Parsons *et al.*, 1993; Sanden *et al.*, 2017; Troeberg *et al.*, 2008). The biomolecular activities of glycosaminoglycans mainly relay on the interaction with proteins, in which molecular weight of glycosaminoglycans is considered an important parameter for their therapeutic effects (Palhares *et al.*, 2021; Wang *et al.*, 2012). Nevertheless, up to the author's knowledge, only limited number of studies have explored the molecular weight-related effects of PPS (Troeberg *et al.*, 2012). In term of chondrogenic properties, it was still unproven that the molecular weight variations in PPS would be associated with differences in their respective treatment effects on chondrocytes.

Notably, chondrocyte dedifferentiation also happens in primary cultures of adult chondrocytes after their released from the ECM (Akaraphutiporn *et al.*, 2020), and in two-dimensional (2D) monolayer cultures, the chondrocytes maintain a fibroblast-like phenotype and change their phenotype-related profiles (Allen *et al.*, 2012; Lin *et al.*, 2008). Therefore, the monolayer culture has several disadvantages for investigating the chondrocyte phenotype changes (Caron *et al.*, 2012; Darling *et al.*, 2005). Besides the monolayer culture, various three-dimensional (3D) culture methods with or without a scaffold have been established to preserve the phenotype and mimic a more cartilage-like environment (Greco *et al.*, 2011; Grigull *et al.*, 2020; Mhanna *et al.*, 2014; Yeung *et al.*, 2019). High-density micro-mass cultures are reproducible and scaffold-free system formed by seeding a high density of cell suspension in a limited space to for a multiple layer structure, which could regulate

chondrocyte phenotype and stimulate the production of the ECM, thereby mimic an *in-vivo*-like environment for the chondrocytes (Anderer *et al.*, 2002; Bassleer *et al.*, 1986; Giovannini *et al.*, 2010; Kuettner *et al.*, 1982). The chondrocyte micro-mass culture system has been proved to be a convenient and reliable experimental tool for studying pharmacological reagents particularly on matrix biosynthesis and degradation (Greco *et al.*, 2011; Thonar *et al.*, 1986). Although the anabolic effects of PPS in chondrocyte have been studied in monolayer cultures, only little evidence has been obtained using these more *in-vivo*-like models.

The objective of this study, therefore, was to investigate properties of PPS on phenotype regulation and ECM production in micro-mass-cultured canine chondrocytes, and to explore the relationship between the effect of PPS and its molecular weight.

2.3 Materials and Methods

2.3.1 Reagents

The reagents used in this study and their sources were as follow: type I collagenase, $NaHCO_3$, penicillin G potassium, streptomycin sulphate, trypsin, DMSO, hydrogen chloride (HCl), and 4% formaldehyde solution were purchased from Wako Pure Chemicals Industries; DMEM was purchased from GIBCO; FBS, RIPA buffer, protease inhibitor cocktail, BSA, Alcian blue, and guanidine hydrochloride were purchased from Sigma-Aldrich; EDTA, HEPES, and MTT, were purchased from Dojindo; BAMBANKER® was purchased from GC LYMPHOTEC; FITC Annexin V Apoptosis Detection Kit I was purchased from BD Biosciences; NucleoSpin RNA Purification Kit and Protein Quantification Assay Kit were purchased from Macherey-Nagel; M-MLV Reverse Transcriptase Kit and NuPAGE™ 4 to 12% Bis-Tris gel were purchased from Invitrogen; KAPA SYBR FAST qPCR Kit was purchased from KAPA Biosystems; Western Blot Ultra-Sensitive HRP Substrate was purchased from Takara Bio Inc.. The culture plates and tubes were purchased from Corning.

Four molecular weights of PPS (Oji Pharma Co.), including 1,500 Da (OJ119A-02), 3,000 Da (OJ119A-03), 5,000 Da (OJ119A-04) and 7,000 Da (OJ119A-05), were used in all experiments. The PPS powdery was dissolved in PBS, then was adjusted to desired concentrations with PBS before adding to the culture medium.

The following antibodies were used in this study: anti-collagen II antibody (Cat. #: ab185430) and anti-SOX9 antibody (Cat. #: ab26414) were purchased from Abcam (Cambridge, U.K.); antibodies against β-actin (Cat. #: 4970), p-Akt (Cat. #: 9271), Akt (Cat. #: 9272), HRP-linked anti-rabbit IgG (Cat. #: 7074) and HRP-linked anti-mouse IgG (Cat. #: 7076) were purchased from Cell Signaling Technology.

2.3.2 Isolation and culture of canine chondrocytes

Five independent canine articular chondrocytes specimens cryopreserved in liquid nitrogen were used for the experiments in this study after recovered. The articular cartilages

were originally harvested from the femoral heads of two client owned dogs: one 12-year-old Labrador retriever received hind limb amputation with the growth of tumor on the distal tibia; one 6-year-old toy poodle received femoral head and neck ostectomy with Legg-Calvè-Perthes Disease. The collection of the cartilage samples was with owners' formal consent. Three cartilage samples were collected from the humerus heads of three experimental beagle dogs' cadavers (two were 3 years old and one was 4 years old) after euthanasia at the end of an unrelated study which did not affect joint structures. Ethical approval for collecting samples from clinic and experimental dogs was obtained from Hokkaido University Institutional Animal Care and Use Committee guidelines (approval number: 12-0059). Harvested cartilages specimens were cut into small fragments. The chondrocytes were released from cartilages by enzymatic digestion at 37°C overnight, using 0.3% type I collagenase in DMEM. Cell suspension was filtered through a membrane and collected into a sterile FALCON® conical tube, then pelleted by a centrifugation at 300×g for 5 min. The chondrocytes were then seeded in 100 mm diameter culture dishes containing 10 mL DMEM with 10% FBS, 10 mM HEPES, 25 mM $NaHCO_3$, 100 Unit/mL penicillin G potassium, and 73 Unit/mL streptomycin sulphate at a cell density of 1.0×10^4 cells/cm^2 and cultured at 37°C in 5% CO_2. The cryopreservation or passage of the chondrocytes were performed when the cell number reached to 80%–90% confluence in the culture plates. For cryopreservation, the chondrocytes detached from the plates using 0.05% trypsin with 0.02% EDTA prepared PBS and subsequently stored with BAMBANKER® in liquid nitrogen. The cryopreservation and recovery of canine chondrocytes were in accordance with manufacturer's instruction.

2.3.3 Cell viability assay

Chondrocytes at the second passage were firstly monolayer cultured in 96-well culture dishes at a density of 2.5×10^4 cells/cm^2 in DMEM with 10% FBS and incubated for 24 hr. Then, the culture medium was changed, and the cells were cultured in the presence (5, 10, 20, 40, 80, and 120 μg/mL) or absence of PPS with different molecular weights for 72 hr. The cell viability of chondrocytes was quantitated by a MTT colorimetric test. Briefly, after a 72 hr incubation with PPS, the culture medium was replaced by 0.5 mg/mL of MTT solution

and incubated for 4 hr. After which, the MTT solution was discharged, and the formazan crystal precipitations in each well were dissolved using 100 μL DMSO. The absorbance at 570 nm was measured by a microplate reader (Multiskan FC) and the reading of all PPS-treated groups was normalized with the control.

2.3.4 Observation of chondrocyte morphology and analysis of cytotoxicity of PPS

Chondrocytes at the second passage were cultured in monolayer as described above and treated with 80 μg/mL of different molecular weights PPS. After a 72 hr incubation, the morphological structures of the chondrocytes were observed and recorded under a light microscope, then the cells were harvested for fluorescent double staining of annexin V and PI using a FITC Annexin V Apoptosis Detection Kit I according to the instruction from the manufacturer. The cytotoxic effects of PPS were measured on a flow cytometer (FACS Verse).

2.3.5 Establishment of chondrocyte micro-mass culture

Chondrocyte micro-mass cultures were established according to a protocol previously described by Greco *et al.* (Greco *et al.*, 2011), with some modification. In short, second-passaged chondrocytes were resuspended in culture medium to adjust the cell number to 2.5×10^7 cells/mL. After which, a 30 μL of cell suspension was gently pipetted to the center of a 12-well culture plate to form a micro-mass. The cells were then incubated for 3 hr at 37°C, 5% CO_2 without increasing volume of the medium to allow the attachment, then 2 mL DMEM with 10% FBS was gently added to the wells before further incubation. The culture medium was changed every 3 days until day 12.

2.3.6 RNA isolation and qPCR

To assess the effects of PPS on the micro-mass-cultured chondrocytes, after a 12-day incubation, the culture medium was change to the fresh medium supplemented with 0, 5, 10, and 40 μg/mL of various molecular weight PPS. The micro-masses were then incubated for 72 hr. Total RNA was extracted from the cells with a NucleoSpin RNA Purification Kit

following the manufacturer's instruction, and the concentration of RNA was measured a by spectrophotometer at 260 nm. The reverse transcription PCR of 1 μg total RNA was performed using M-MLV Reverse Transcriptase Kit according to manufacturer's protocol. Fold changes of the expression levels of target genes were evaluated by a two-step qPCR method using a KAPA SYBR FAST qPCR Kit, with standard curves to normalize the efficiency of primers between reactions. *COL2A1*, *ACAN*, *SOX9*, and *COL1A2* mRNA levels were used to identify the phenotypic changes of the chondrocytes, and the *GAPDH* gene was used as a reference gene to normalization the expression levels of all target genes. The information of the primers is shown in Table 3.

2.3.7 Protein extraction and Western blot

The treatment for chondrocyte micro-mass cultures was described in the section of RNA isolation. Micro-mass cultures were washed, then lysed with chill RIPA buffer supplemented with protease inhibitor cocktail in a 1:100 dilution. The cell lysates were centrifuged at 13,000×g for 20 min at 4°C and supernatants were recovered to new collection tubes. Total protein concentration was checked with a Protein Quantification Assay Kit. Four microgram total protein of each sample was separated by sodium dodecyl sulfate–polyacrylamide gel electrophoresis with a 4 to 12% NuPAGE™ Bis-Tris gel, then transferred onto a PVDF membrane. The Membranes were then blocked with 3% BSA-PBST solution for 1 hr. After which, the membranes were incubated with primary antibodies (dilution factor: 1:800 for p-Akt; 1:1,500 for collagen II, SOX9, and Akt; 1:4000 for β-actin) overnight at 4°C, then incubated with secondary antibodies (dilution factor: 1:2,000 for phospho-Akt; 1:4,000 for collagen II, SOX9, and Akt; 1:8,000 for β-actin) for 1 hr. The membranes were incubated with Western Blot Ultra-Sensitive HRP Substrate for 5 min to develop the bands. The chemiluminescence was visualized using Image Quant LAS 4000 system. Intensity of the bands was quantified by ImageJ software. The protein productions were normalized by β-actin, while p-Akt values were normalized by Akt protein.

2.3.8 Identification of ECM formation by Alcian blue staining

After cultured in micro-mass for 12 days, the chondrocytes were treated with 0, 10 and 40 μg/mL of four molecular weights PPS for 72 hr. Alcian blue staining was performed to check the deposition of proteoglycans in the micro-masses (Buee *et al.*, 1991). Briefly, after discharged the culture medium, chondrocytes were gently washed with PBS for three times and fixed with 4% formaldehyde solution for 30 min. The micro-masses were then rinsed with PBS and stained with 1% Alcian blue prepared in 0.1 mol/L HCl for 30 min. After which, the staining solution was removed, and each micro-mass was washed three time with 0.1 N HCl and one time with distilled water. The micro-masses were observed on visual and microscopic inspection to check the blue staining. The proteoglycans deposited in the micro-masses was then quantified according to a protocol previously described (Griffin *et al.*, 2017). Briefly, the color was dissolved in 6 M guanidine hydrochloride overnight at room temperature, then collected in to a 96-well plate. The absorbance was measured at 595 nm.

2.3.9 Statistical analysis

Statistical analysis of quantitative results was conducted by GraphPad Prism software version 9.2.0. Statistical comparisons were performed using ANOVA. When a significant difference was observed, a Dunnett's test was then performed to compare between the treatment groups and the control. Pearson correlation coefficient was used to calculate the correlation between PPS molecular weight and the cell viability, gene expression levels, or proteins productions, respectively. Quantitative results are shown as means ± SDs, and significant difference was considered as $p < 0.05$.

Table 3. Primers used to evaluate gene expression levels in micro-mass-cultured chondrocytes.

Gene symbol	Primer sequence	Domain	Amplicon (bp)	Accession
GAPDH	Forward: 5′-CTGAACGGGAAGCTCACTGG-3′	664–683	129	NM_001003142.2
	Reverse: 5′-CGATGCCTGCTTCACTACCT-3′	792–773		
COL1A2	Forward: 5′-GTGGATACGCGGACTTTGTT-3′	150–169	164	NM_001003187.1
	Reverse: 5′-GGGATACCATCGTCACCATC-3′	313–294		
COL2A1	Forward: 5′-CACTGCCAACGTCCAGATGA-3′	4127–4146	215	NM_001006951.1
	Reverse: 5′-GTTTCGTGCAGCCATCCTTC-3′	4341–4322		
ACAN	Forward: 5′-ACTTCCGCTGGTCAGATGGA-3′	6566–6585	111	NM_001113455.3
	Reverse: 5′-TCTCGTGCCAGATCATCACC-3′	6676–6657		
SOX9	Forward: 5′-GCCGAGGAGGCCACCGAACA-3′	565–583	179	NM_001002978.1
	Reverse: 5′-CCCGGCTGCACGTCGGTTTT-3′	743–724		

GAPDH = glyceraldehyde-3-phosphate dehydrogenase, *COL1A2* = collagen type I alpha 2 chain, *COL2A1* = collagen type II alpha 1 chain, *ACAN* = aggrecan, *SOX9* = SRY-Box transcription factor 9.

2.4 Results

2.4.1 PPS reduced the viability of chondrocytes

The results of MTT assay (Figure 6) indicated that the chondrocyte viability was reduced in a concentration-dependent manner after exposed to different molecular weight PPS for 72 hr. Significant reduction was firstly shown in the cultures incubated with 7,000 Da PPS at 10 μg/mL (p = 0.002), and all of the four molecular weights of PPS exhibited significant inhibitory effect at 120 μg/mL (p = 0.002 with 1,500 Da, and p < 0.001 with others). Significant negative correlations were found between molecular weights of PPS and chondrocyte viabilities from a concentration of 20 μg/mL (Table 4).

2.4.2 Effects of PPS on the morphological appearance of chondrocytes in monolayer

After incubated with various molecular weights of PPS at 80 μg/mL for 72 hr, reduced cell confluence was observed in monolayer cultures exposure to PPS with 5,000 and 7,000 Da compared with the non-treated group (Figure 7A). However, no clearly morphological changes were identified between the groups (Figure 7B), and the chondrocytes in all groups maintained a fibroblast-like shape.

2.4.3 All molecular weight of PPS has no cytotoxic effect on chondrocytes

The cytotoxic assay of PPS by flow cytometry showed a similar distribution of the chondrocytes was found between the groups treated with different molecular weights of PPS at 80 μg/mL and the control (Figure 8). The percentage of live and dead cells showed no significant difference between all treatment groups and the non-treated group (Table 5).

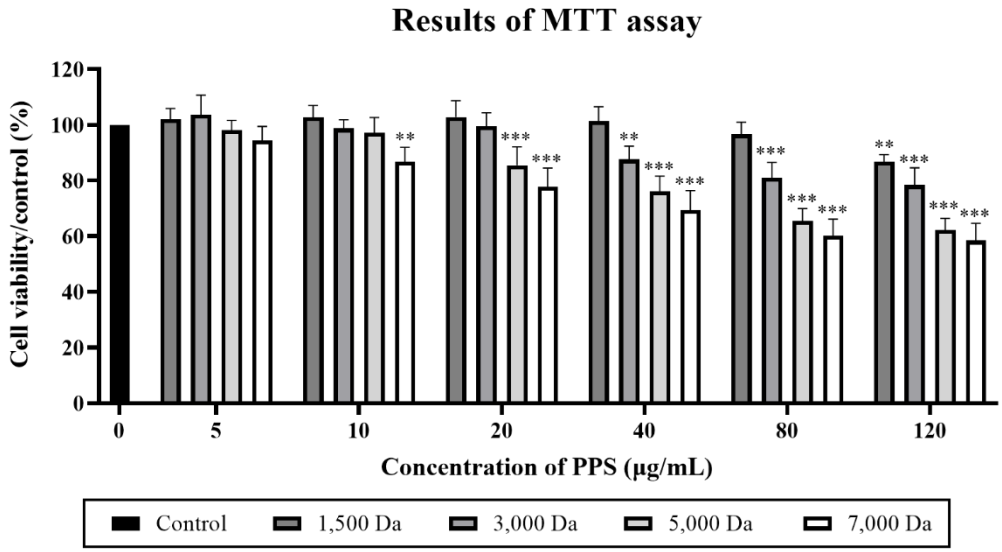

Figure 6. Viability of chondrocytes was decreased with PPS treatment.

Chondrocytes were seeded as a monolayer in 96-well plates for 24 hr prior to the treatment with various molecular weight of PPS (1,500, 3,000, 5,000, and 7,000 Da) at different concentration (0, 5, 10, 20, 40, 80, and 120 μg/mL) for 72 hr. The cell viability was analyzed by MTT assay after PPS treatment. Data represents the mean ± SDs of five independent experiments (*$p < 0.05$, **$p < 0.01$, and ***$p < 0.001$, compared with 0 μg/mL of PPS).

Table 4. Correlation between PPS molecular weight and cell viability of monolayer-cultured chondrocytes.

	At 5 μg/mL	**At 10 μg/mL**	**At 20 μg/mL**
r	-0.718	-0.857	-0.923
95% confidence interval	-0.980 to 0.448	-0.990 to 0.102	-0.995 to -0.221
p (two-tailed)	0.172	0.063	0.025[a]
	At 40 μg/mL	**At 80 μg/mL**	**At 120 μg/mL**
r	-0.970	-0.979	-0.981
95% confidence interval	-0.998 to -0.608	-0.999 to -0.706	-0.999 to -0.729
p (two-tailed)	0.006[a]	0.004[a]	0.003[a]

a. $p < 0.05$ indicates a significantly difference.

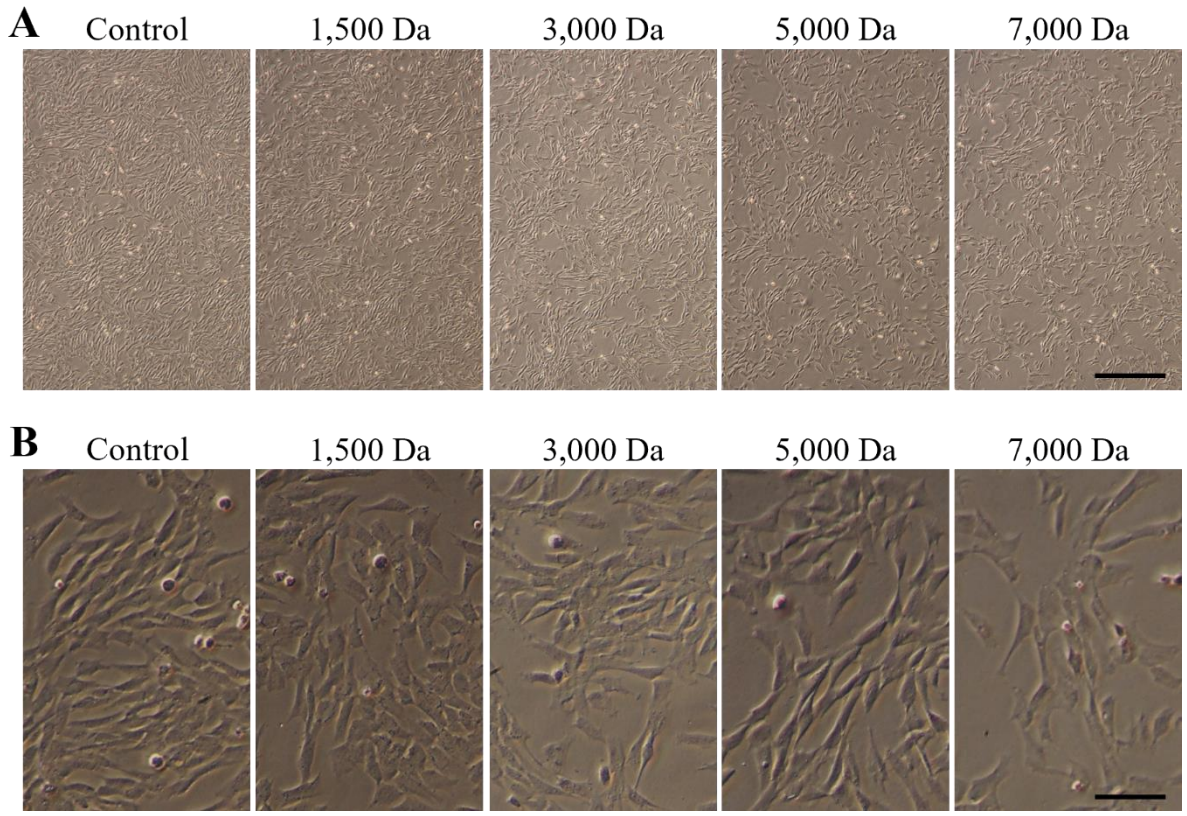

Figure 7. Morphological appearance of the monolayer-cultured chondrocytes under a light microscope.

Canine chondrocytes were cultured for 24 hr and then treated with various molecular weight (1,500, 3,000, 5,000, and 7,000 Da) of PPS at 80 μg/mL for 72 hr. Lower confluent of the cells can be seen with higher molecular weights PPS. (A) Scale bar: 500 μm. (B) Scale bar: 100 μm.

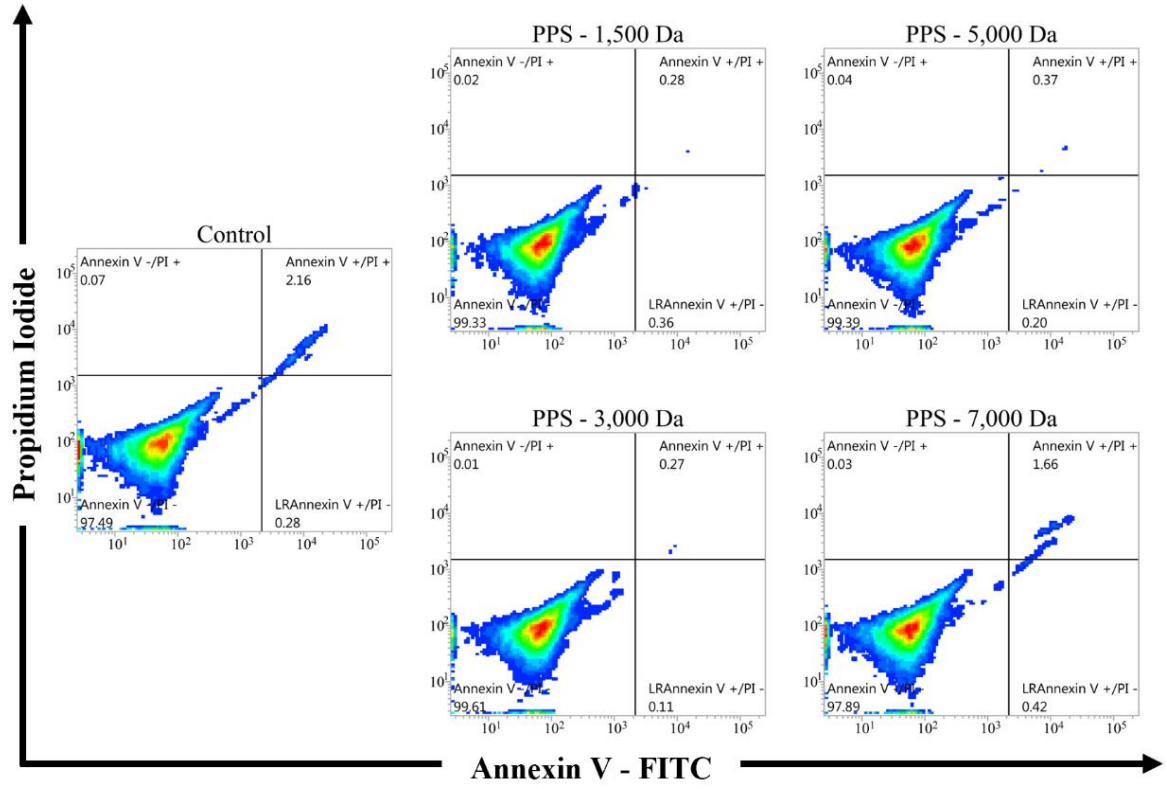

Figure 8. Treatment with PPS did not induce cytotoxic effect in chondrocytes.

Chondrocytes were cultured in monolayer for 24 hr prior to the exposure with various molecular weight of PPS (1,500, 3,000, 5,000, and 7,000 Da; concentration: 80 μg/mL). Chondrocyte apoptosis was evaluated by flow cytometry detection with annexin V and PI staining. Upper left quadrant: necrotic cells; upper right quadrant: late apoptotic cells; lower left quadrant: live cells; and lower right quadrant: early apoptotic cells.

Table 5. Percentage of cells binding to annexin V and PI in each quadrant.

	Annexin V -/PI -	Annexin V +/PI -	Annexin V -/PI +	Annexin V +/PI +
	Live cells	**Early apoptotic cells**	**Necrotic cells**	**Late apoptotic cells**
Control	95.27 ± 2.12	1.10 ± 1.14	0.02 ± 0.03	3.61 ± 1.87
1,500 Da	95.96 ± 2.17	1.07 ± 1.14	0.04 ± 0.03	2.94 ± 1.52
3,000 Da	96.05 ± 2.84	1.12 ± 1.43	0.04 ± 0.03	2.78 ± 1.76
5,000 Da	96.21 ± 2.23	0.89 ± 0.98	0.03 ± 0.04	2.87 ± 1.70
7,000 Da	94.99 ± 1.99	1.17 ± 0.85	0.06 ± 0.05	3.77 ± 1.37

No statistical significance was found between the control and each treatment group in all quadrants. Data represent means ± SDs of five independent experiments.

2.4.4 PPS promotes the expression of chondrogenic phenotype related genes

The results of qPCR revealed significant upregulation of the expression levels of two cartilage-specific genes, *COL2A1* and *ACAN*, in micro-mass cultured canine chondrocytes after incubated with 7,000 Da PPS at 10 (p = 0.012 for *COL2A1* and p = 0.011 for *ACAN*) and 40 μg/mL (p < 0.001 for *COL2A1* and p < 0.001 for *ACAN*) for 72 hr when compared with the control (Figure 9A and B). A significant upregulation of the *COL2A1* and *ACAN* gene expression levels was also confirmed in 5,000 Da PPS group at higher concentrations. Moreover, the mRNA level of *SOX9* was significantly upregulated after exposure to PPS of 5,000 (p = 0.031), and 7,000 Da (p < 0.001) at 40 μg/mL (Figure 9C), compared with the control, respectively. Nevertheless, *COL2A1* and *SOX9* gene expression in the 1,500 Da PPS-treated group remained unchanged at all concentrations (Figure 9A and C), while a concentration-dependent trend was identified with the treatment of other three molecular weight of PPS. Notably, strong positive correlations between the molecular weight of PPS and mRNA levels of *COL2A1* (r = 0.956, p = 0.011 at 10 μg/mL; and r = 0.937, p = 0.019 at 40 μg/mL), *ACAN* (r = 0.975, p = 0.005 at 10 μg/mL; and r = 0.982, p = 0.003 at 40 μg/mL), and *SOX9* (r = 0.906, p = 0.034 at 10 μg/mL; and r = 0.968, p = 0.007 at 40 μg/mL) were confirmed noticed at higher concentration (Table 6). One interesting finding of the qPCR results was the upregulation (p = 0.001) of *COL1A2* level in chondrocytes exposed to 40 μg/mL of 7,000 Da PPS at 72 hr (Figure 9D), which the expression of this gene was slightly decreased in the groups of lower molecular weight.

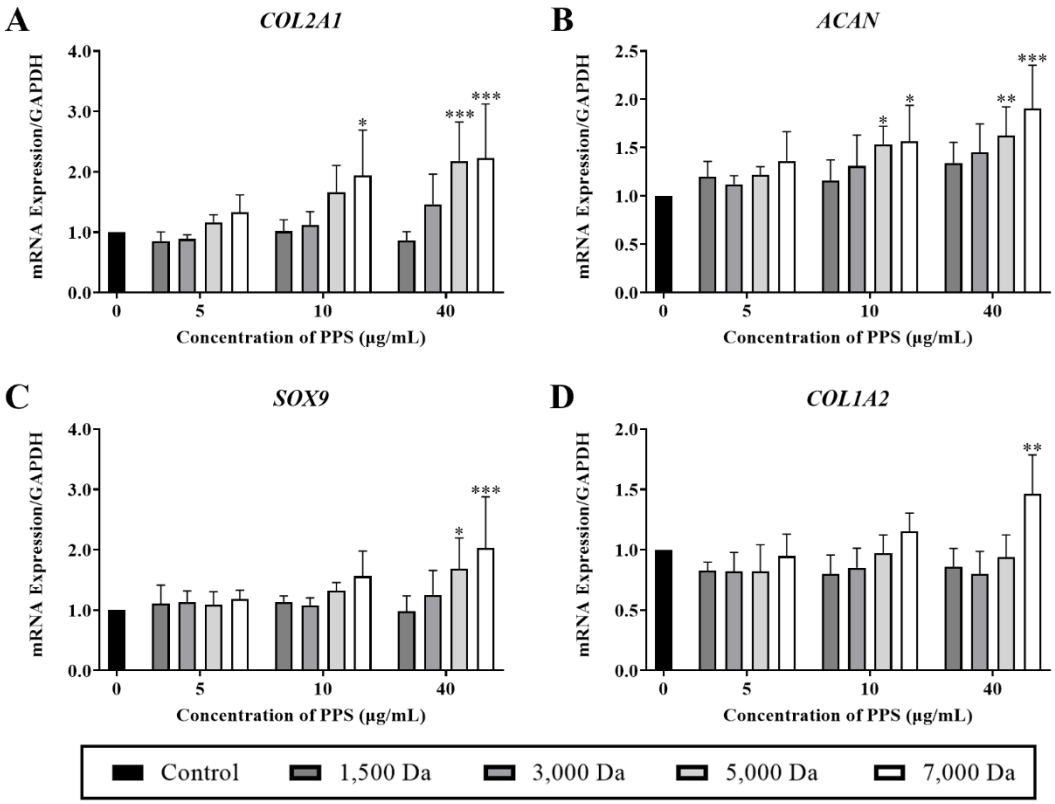

Figure 9. Higher molecular weights of PPS upregulated the expression levels of hyaline cartilage-specific gene markers.

After micro-mass-cultured for 12 days, the chondrocytes were incubated with 1,500, 3,000, 5,000, and 7,000 Da of PPS at 0, 5, 10, and 40 μg/mL for 72 hr. The mRNA levels of were evaluated by qPCR. The expression levels of (A) *COL2A1*, (B) *ACAN*, and (C) *SOX9* genes were increased with the PPS treatment in a same manner, while (D) *COL1A2* expression level only significantly upregulated with 7,000 Da PPS at the highest concentration. Data are the means ± SDs of five independent experiments (*$p < 0.05$, **$p < 0.01$, and ***$p < 0.001$, compared with 0 μg/mL of PPS).

Table 6. Correlation between the molecular weight of PPS and the expression levels of target genes.

	At 5 μg/mL	At 10 μg/mL	At 40 μg/mL
COL2A1			
r	0.814	0.956	0.937
95% confidence interval	-0.242 to 0.987	0.470 to 0.997	0.314 to 0.996
p (two-tailed)	0.094	0.011[a]	0.019[a]
ACAN			
r	0.895	0.975	0.982
95% confidence interval	0.059 to 0.993	0.668 to 0.998	0.749 to 0.999
p (two-tailed)	0.040[a]	0.005[a]	0.003[a]
SOX9			
r	0.823	0.906	0.968
95% confidence interval	-0.216 to 0.988	0.117 to 0.994	0.588 to 0.998
p (two-tailed)	0.087	0.034[a]	0.007[a]
COL1A2			
r	-0.142	0.599	0.659
95% confidence interval	-0.910 to 0.846	-0.601 to 0.969	-0.533 to 0.975
p (two-tailed)	0.820	0.286	0.226

COL2A1 = collagen type II alpha 1 chain, *ACAN* = aggrecan, *SOX9* = SRY-Box transcription factor 9, and *COL1A2* = collagen type I alpha 2 chain.

a. $p < 0.05$ indicates a significantly difference.

2.4.5 PPS increases the synthesis of collagen II and SOX9 protein and downregulates phosphorylation of Akt in micro-mass cultured chondrocytes

Western blotting analysis was used to evaluate the production of collagen II and SOX9 protein and the activation of Akt pathway (Figure 10A) in micro-mass-cultured chondrocytes. After 72 hr incubated with PPS, the protein production of collagen II in treatment groups was concentration and molecular weight-dependently enhanced (Figure 10B). The largest fold change was shown in 5,000 Da group at 40 μg/mL ($p < 0.001$). Other significant increase was observed with 3,000 Da PPS at 40 μg/mL ($p = 0.002$), with 5,000 Da PPS at 10 μg/mL ($p = 0.032$), and with 7,000 Da PPS at 10 ($p = 0.002$) and 40 ($p = 0.002$) μg/mL, compared with the non-treated group, respectively. Collagen II protein production was positively correlated with PPS molecular weight at 10 μg/mL ($r = 0.991$, $p = 0.001$), although no correlation was found at 40 μg/mL (Table 7). Furthermore, SOX9 protein production was significantly increased with 5,000 Da ($p = 0.030$) and 7,000 Da ($p = 0.002$) PPS treatment at 40 μg/mL, compared with the control (Figure 10C). Positive correlations between PPS molecular weight and SOX9 protein level were detected at 10 ($r = 0.960$, $p = 0.001$) and 40 ($r = 0.983$, $p = 0.003$) μg/mL (Table 7). In contrast with collagen II and SOX9 protein, the phosphorylation of Akt was inhibited by PPS with higher molecular weights (Figure 10D). The p-Akt/Akt ratio was significantly reduced with 7,000 Da PPS at 40 μg/mL ($p = 0.022$), and a negative correlation was identified between PPS molecular weight and Akt phosphorylation at 40 μg/mL ($r = - 0.997$, $p < 0.001$; Table 7).

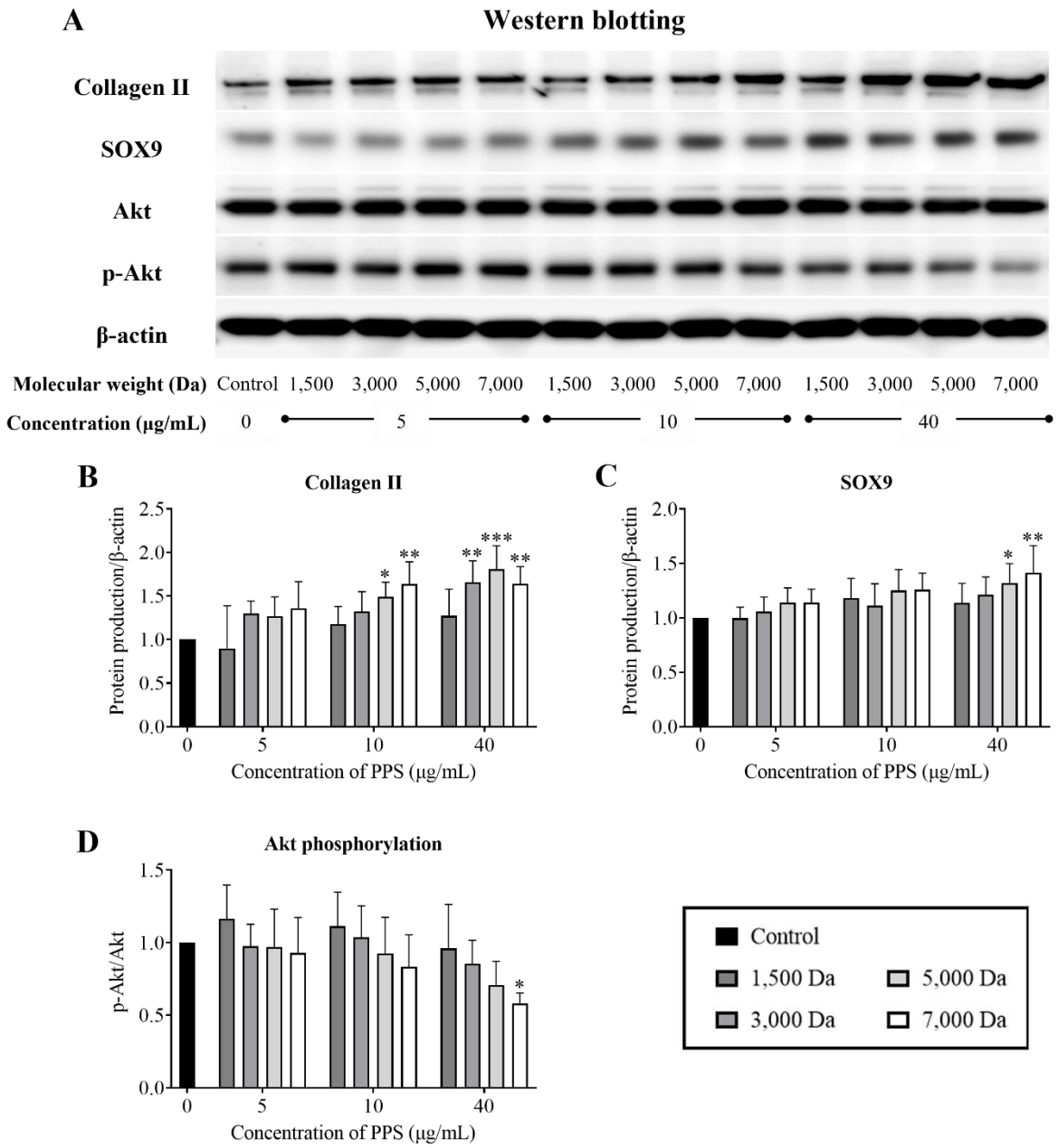

Figure 10. PPS stimulated collagen II and SOX9 protein productions and inhibited Akt phosphorylation in micro-mass-cultured chondrocytes.

(A) Total protein in the chondrocytes was analyzed by Western blotting. Twelve-day micro-mass cultures were exposed to four molecular weights of PPS (1,500, 3,000, 5,000, and 7,000 Da) at 0, 5, 10, and 40 μg/mL. Protein production of (B) collagen II was significantly increased with higher molecular weights PPS. (D) Akt phosphorylation was significantly reduced with PPS of 7,000 Da at 40 μg/mL. Data are the means ± SDs of five independent experiments (*$p < 0.05$, **$p < 0.01$, and ***$p < 0.001$).

Table 7. Correlation between PPS molecular weight and protein productions.

	At 5 µg/mL	At 10 µg/mL	At 40 µg/mL
Collagen II			
r	0.865	0.991	0.835
95% confidence interval	-0.072 to 0.991	0.857 to 0.999	-0.181 to 0.989
p (two-tailed)	0.058	0.001[a]	0.079
SOX9			
r	0.960	0.824	0.983
95% confidence interval	0.506 o 0.997	-0.215 o 0.988	0.764 to 0.999
p (two-tailed)	0.001[a]	0.087	0.003[a]
p-Akt/Akt			
r	-0.652	-0.837	-0.997
95% confidence interval	-0.974 to 0.542	-0.989 to 0.174	-1.000 to -0.947
p (two-tailed)	0.233	0.077	< 0.001[a]

a. $p < 0.05$ indicates a significantly difference.

2.4.6 Higher molecular weight of PPS increases proteoglycans deposition in micro-mass culture of chondrocytes

Accumulation of proteoglycans in the ECM of chondrocyte micro-masses were detected by Alcian blue staining. After 72 hr incubated with different molecular weights PPS at 0, 10, and 40 μg/mL, increased blue staining were confirmed in all treatment groups (Figure 11A and B). Stronger staining was detected in 5,000 and 7,000 Da group compared with the lower molecular weight PPS groups and the control. The semi-quantitative results showed that the optical density was significantly increased at 595 nm with 7,000 Da PPS treatment at 10 μg/mL (p = 0.030), and with 5,000 Da (p = 0.048) and 7,000 Da (p = 0.004) treatments at 40 μg/mL (Figure 11C). These results indicated that higher molecular weights of PPS strongly stimulated the ECM production of canine chondrocytes.

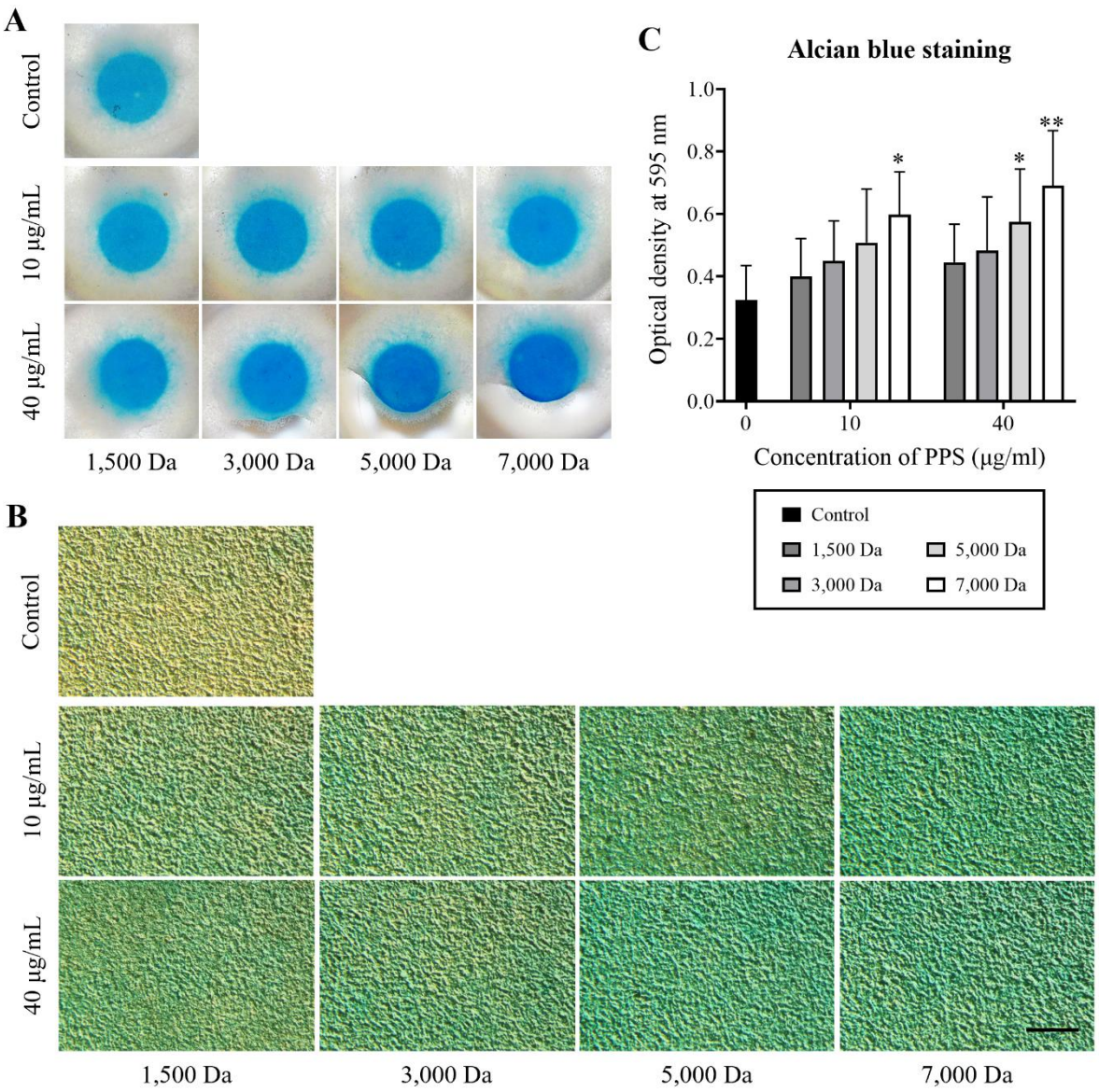

Figure 11. PPS with higher molecular weight promoted proteoglycans accumulation in chondrocyte micro-mass cultures.

Chondrocytes were cultured in micro-masses for 12 days, following the treatment with various molecular weights of PPS (1,500, 3,000, 5,000, and 7,000 Da) at 0, 10, and 40 μg/mL for 72 hr. The images of the micro-masses were (A) observed on culture plates and (B) observed under a light microscope. Stronger Alcian blue staining was observed in 5,000 Da and 7,000 Da groups. (B) Scale bar: 100 μm. (C) The absorbance at 595 nm was significantly increased following 5,000 and 7,000 Da PPS treatments at 40 μg/mL. Data are the means ± SDs of five independent experiments (*$p < 0.05$ and **$p < 0.01$, compared with 0 μg/mL PPS).

2.5 Discussion

The results of MTT colorimetric assay indicated that PPS reduced the viability of canine chondrocytes in a concentration-dependent pattern at 72 hr of treatment, which higher molecular weight of PPS provided stronger effect at higher concentration. Decreased cell number with higher molecular weight of PPS was evidenced by micrographs at 80 μg/mL. However, no morphological sign of cell death was found under microscopes. The Flow cytometry with by annexin V and PI staining also demonstrated no increased proportion of dead cells in the monolayer cultures after incubated with 80 μg/mL of PPS for 72 hr in all group. According to these results, despite reducing cell viability in MTT assay, PPS up to a molecular weight of 7,000 Da has no cytotoxic effects in canine chondrocytes even at high concentration. This finding is coincident with other related studies showing the safety of high concentration of PPS on chondrocytes (Bwalya *et al.*, 2018; Bwalya *et al.*, 2017a; Ghosh, 1999; Sunaga *et al.*, 2012). One possibility for the decreased absorbance in MTT and cell number observed in the present study is that treatment of PPS inhibits the proliferation of chondrocytes, since previous studies verified high concentration of PPS increases the percentage of cells in G1 phase and decreases the percentage of cells in S phase in term to reduce the proliferative activities on chondrocytes (Akaraphutiporn *et al.*, 2020). In addition, the lower proliferative activities of chondrocytes are proved to inversely relates the synthetic activities of the ECM (Akaraphutiporn *et al.*, 2020; Otero *et al.*, 2012).

Chondrogenic effects of PPS on chondrocytes were investigated using a micro-mass culture system. To understand how PPS regulates chondrogenic profile, this study evaluated the expression of phenotype related markers in canine chondrocytes. In agree with previous studies (Akaraphutiporn *et al.*, 2020; Bwalya *et al.*, 2018; Ghosh *et al.*, 2010), the qPCR results validate the expression levels of cartilage-specific gene markers, *COL2A1* and *ACAN*, were upregulated with the treatment of PPS, evidencing the promotion of a chondrogenic phenotype in dedifferentiated chondrocytes (Lin *et al.*, 2008). However, it should be notice that the statistical significance was only confirmed in the 5,000 and 7,000 Da PPS groups in the current study. Consistent with *COL2A1* gene expression, protein production of collagen

II in chondrocytes was enhanced with PPS treatment in a molecular weight-dependent manner at higher concentration and the highest level was found with PPS of 5,000 Da at 40 μg/mL. Similarly, PPS encouraged the deposition of proteoglycans at higher concentration, and higher molecular weight PPS (5,000 and 7,000 Da) provided a stronger effect than lower molecular weights (1,500 and 3,000 Da) PPS. The transcription SOX9 is recognized as a decisive transcript factor in cartilage biosynthesis, which is essential for activating the expression of several chondrocyte-specific genes and regulates chondrocyte differentiation (Akiyama *et al.*, 2004; Gao *et al.*, 2014; Takahashi *et al.*, 1998). During the *in-vitro* culture of chondrocytes, the SOX9 level has been found decreased with the increase of passage (Lin *et al.*, 2008; Parreno *et al.*, 2017), while using 3D cultures could stimulate the production of SOX9, with upregulation of other cartilage-specific markers in the chondrocytes (Bernstein *et al.*, 2009; Caron *et al.*, 2012). This study showed that after 72 hr treatment with PPS, the gene expression and protein production of SOX9 in micro-mass-cultured chondrocytes were concentration-dependently and molecular weight-dependent upregulated, which corresponded with the expression levels of *COL2A1* and *ACAN* genes. In summary, these results suggested that PPS treatment effectively promoted a chondrogenic phenotype in dedifferentiated chondrocytes and enhanced the biosynthesis of chondrocyte ECM.

One provocative finding in this study is the upregulated expression of *COL1A2*, the fibroblastic marker in canine articular chondrocytes, with the treatment of 7,000 Da PPS. Other molecular weights of PPS did not induce this increase of *COL1A2* mRNA level. Previous studies have evidenced that collagen type I and type II production of human chondrocytes culture upregulated simultaneously in alginate-bead and pellet cultures, however, the authors attributed this phenomenon to the osteoarthritic nature of their cell sources (Caron *et al.*, 2012). Another study reported a similar finding, which mRNA expression of *COL1A2* was massively increased with treatment of a different type of polysaccharide, polysulfated glycosaminoglycan (molecular weight ranged from 3,000 to 15,000 Da) in canine MSCs, while PPS with an average molecular weight between 4,000 and 6,000 Da showed no significant effect on the *COL1A2* mRNA level (Bwalya *et al.*,

2017b). Possibly the high molecular weight of PPS is the main factor in this fibrocartilaginous phenotype in the culture.

Phosphorylation of Akt in chondrocyte micro-mass culture was clearly suppressed at the highest concentration of PPS with higher molecular weights in this study. Nevertheless, the role of the PI3K/Akt signaling pathway in the phenotype change of chondrocyte is still under discussion. Previously, some studies have demonstrated that the PI3K/Akt pathway positively contributes on the hypertrophic process of chondrocytes (Fujita *et al.*, 2004; Ulici *et al.*, 2008). In contrast, other studies pointed out that activates PI3K/Akt pathway inhibits the terminal differentiation of human chondrocytes (Kita *et al.*, 2008). Nevertheless, increased mRNA and protein levels of collagen II and SOX9 by pharmacological treatment were found negatively corresponded with the phosphorylation of Akt in chondrocytes in a previous study (Liu *et al.*, 2020). Although the exact function of the PI3K/Akt signaling pathway is blurred, the results of increased cartilage-specific markers and ECM productions in the present study suggested that suppressing phosphorylation of Akt could relates to a beneficial effect of PPS in promoting chondrocyte redifferentiation.

PPS is a low molecular weight semisynthetic anionic polysaccharides that shares a similar structure with heparins or other naturally sulfated glycosaminoglycans (Alekseeva *et al.*, 2020; Parsons *et al.*, 1993). The biological activities of glycosaminoglycans depend predominantly on their interaction of proteins (Palhares *et al.*, 2021), and the highly native charged feature is thought to be one of the key factors in binding of glycosaminoglycans to proteins (Meneghetti *et al.*, 2015; Wang *et al.*, 2012). Molecular weight is an important parameter with therapeutic application of glycosaminoglycans, for changing of saccharide units affects the density of charge and binding sites. In term of glycosaminoglycans with small molecular mass, previous research has shown that heparin fractions (ranged from 1,700 to 12,000 Da) with higher molecular weight were more effective in inhibition of aggrecanase I activity (Mousa, 2005). Studies on PPS suggested the affinity between ADAMTS5 and its endogenous inhibitor, TIMP3 was increased by PPS through formation of a tri-molecular complex, which longer PPS chain provided stronger effects (Troeberg *et*

al., 2012). While previous studies focused on the specific enzymes, the present study demonstrated for the first time that larger molecular weights of PPS were more effective at improving the chondrogenic abilities on chondrocytes. Four different molecular weights of PPS were tested in the current study, which 7,000 Da PPS provided the strongest effects. PPS with 1,500 Da was less effective on regulation of chondrocyte phenotype, which in line with previous findings for PPS binding to proteins, with an average length of 11 monosaccharides (3,300 Da) was 100-fold more effective than PPS of 8 monosaccharides (2,400 Da) (Troeberg *et al.*, 2012). It must be mentioned that in this study, significantly increased of *SOX9*, *COL2A1*, and *ACAN* gene expression and ECM productions in the chondrocytes can also be seen in 5,000 Da PPS groups at higher concentrations, which indicated that this molecular weight of PPS maybe sufficient to achieve these treatment effects in canine chondrocytes.

Several limitations should be noticed in this study, including the small sample scale of five cartilage samples. Although the results suggest that PPS could protect chondrogenic phenotypes via suppressing Akt pathway, upper stream regulators were not identified in this study. Furthermore, the effects of different molecular weights of PPS were compared only through chondrocyte phenotypic changes, and the interactions between PPS and cells were not explored. Considering the complex structure of cells, a reliable tracing technique is need in the next for digging the underlying mechanism for structure-function relation of PPS.

In conclusion, this study demonstrated that PPS promotes chondrogenic phenotypes and improves the quality of ECM in canine chondrocytes in an *in-vivo*-like micro-mass cultured condition. The suppression of Akt signal pathway with PPS treatment appears to be related with the phenotype-protective properties of PPS. These findings about the phenotype shift could deepen our understanding of chondrocyte physiologies and may provide a new target for OA treatment. A molecular weight-dependent effect of PPS on chondrocytes was also confirmed in this study, which larger PPS molecules (5,000 and 7,000 Da) generate stronger effects in stimulating the expression of cartilage-specific markers at same concentration. Besides the increased *COL1A2* expression by 7,000 Da PPS rises a concern of

fibrocartilaginous ECM formation, PPS up to 7,000 Da does not produce detectable cytotoxic effect in canine chondrocytes even at a high concentration. The relation between the structure and the function of PPS in chondrocytes phenotypic change and ECM productions in the present study suggested that increasing the molecular weight of PPS could enhance its therapeutic effects in OA chondrocytes.

General Discussion

Articular cartilage consists of specialized cells called chondrocytes within a large amount of ECM. Despite their small population in the cartilage, chondrocytes play a critical role in maintaining the homeostasis of ECM composition under normal conditions (Fox *et al*., 2009). Physiologically, chondrocytes are quiescent in articular cartilage and exhibit very low proliferative and synthetic activities. However, in the early stages of OA, chondrocytes experience a phenotype change and transiently increase their proliferative activity, which alters the synthesis of ECM components in chondrocytes and upregulates the production of several cartilage catabolic mediators (Charlier *et al.*, 2019; Chen *et al.*, 2021; Pearle *et al*., 2005). Since chondrocytes are the only resident cell type, their phenotypic change is primarily responsible for the progression of OA in the cartilage. Interventions of this process could contribute to the development of treatments for OA.

Pentosan polysulfate sodium is a semi-synthetic polysaccharide derived from European beechwood, and has been used to relieve the clinical symptoms of thrombi and interstitial cystitis in humans. In the past decades, studies have demonstrated that PPS reduces articular cartilage destruction of during process in horses and dogs through suppressing cytokine-activated signaling pathway, downregulating the production of OA-related mediators, and inhibiting the activity of proteases degrading cartilage components (Bwalya *et al*., 2017a; Ghosh *et al.*, 2005; Kumagai *et al.*, 2010; Sunaga *et al.*, 2012). Recent studies have shown PPS could stimulate the chondrogenic differentiation of canine and human MSCs (Bwalya *et al.*, 2017b; Ghosh *et al.*, 2010). PPS has also been found to stimulate the redifferentiation of cultured chondrocytes, which would be features of phenotypic changes, and promote chondrocyte ECM synthesis (Akaraphutiporn *et al.*, 2020). However, the underlying mechanism of these anabolic effects of PPS needs further exploration. On the other hand, the structure similarity between PPS and glycosaminoglycans has been identified. Glycosaminoglycans achieve their biological effects through the interaction between their negatively charged sulfate groups and proteins. Thus, altering the molecular weight or sulfate level of glycosaminoglycans can affect their ability to bind to proteins, which in turn changes their therapeutic effects (Linhardt *et al.*, 2004; Mizumoto *et al.*, 2015; Xu *et al.*,

2014). Although previous studies have demonstrated the structure-effect relationship of several glycosaminoglycans, this property of PPS is poorly understood. The present study was therefore, designed to investigate regulatory effects of PPS on cell proliferation and cell cycle progression of chondrocytes, and to explore its properties to promote the redifferentiation and ECM production of *in-vitro* cultured canine articular chondrocytes. The structure-dependent effects of PPS on these aspects were investigated using two series of PPS products: one differing in sulfated level, and the other differing in molecular weight. The major findings of the present study can be summarized into two sections:

In section one, the effects of PPS with four different sulfate levels (0, 5, 16, and 19% as full sulfate) on the proliferative activity and its related phenotype change of monolayer-cultured canine chondrocytes was investigated. The results demonstrated that full sulfate PPS reduced chondrocyte proliferative activity through suppressing the progression of cell cycle from G1 phase to later phases, which was supported by the downregulated gene expression of *CDK4* and *CCND1*. In addition, PPS upregulated the mRNA levels of *COL2A1* and *SOX9*, indicating the promotion of chondrogenic phenotype in chondrocytes. The results of Western blotting further suggested that PPS inhibited chondrocyte proliferation and promoted chondrogenic phenotype by targeting the PI3K/Akt signaling pathway. Notably, only PPS with full sulfate level exerted significant effects, while lower sulfate level PPS showed weaker or no effects in all the experiments. The findings indicate that PPS could be beneficial in regulating the phenotypic changes of chondrocytes, and the full sulfate level of PPS may be necessary to achieve these effects.

In the second section, a micro-mass culture model was applied to investigate PPS with four different molecular weight (1,500, 3,000, 5,000, and 7,000 Da) on promoting the redifferentiation and ECM production of canine chondrocytes. The results of gene expression and protein production indicated that PPS with higher molecular weight clearly promoted the redifferentiation of micro-mass-cultured chondrocytes through inhibiting Akt pathway. Furthermore, the proteoglycan deposition in chondrocyte ECM in micro-masses was also improved after incubated with PPS. Interestingly, the effects of PPS in promoting

the redifferentiation and ECM production were positive correlated with the molecular weight of PPS, in which 5,000 and 7,000 Da PPS exerted stronger treatment effects. Although all four types of PPS did not exert cytotoxic effect, the increased expression of a fibroblast marker after exposure to 7,000 Da PPS does raise the concern about unfavorable effects of higher molecular weight PPS. All in all, this study confirmed that PPS could promote the redifferentiation and ECM synthesis of dedifferentiated articular chondrocytes, which increase the molecular weight of PPS could enhance these properties.

As traditional treatments for OA can only alleviate clinical symptoms, the needs for drugs that can control the pathogenesis of OA are growing (Ghouri *et al.*, 2019; Mobasheri, 2013). PPS is one of the few DMOADs which have shown therapeutic effects on both the progressive inflammatory condition as well as degenerative structural changes of OA (Oo *et al.*, 2022). The dedifferentiation-related changes of chondrocytes could be observed in OA cartilages especially during the early stage, which contributes to the disease progression of OA and raise a challenge for repairing the structural damage of cartilages. This study demonstrates the potential of PPS to reverse this phenomenon, and explored the involved mechanisms of this effects. The finding could serve as strong evidence to support its effectiveness in clinical trials and provide a promising option for the treatment of OA.

The structure of polysaccharide substances greatly affects its biological. Nevertheless, the structure-effect relationship of PPS was poorly discussed previously. To the author's knowledge, the present study provides the first evidence suggesting the importance of full sulfate level for PPS in chondrocytes. Given that the sulfation process of PPS is exhaustive and non-selective (Alekseeva *et al.*, 2020), reducing PPS sulfate level may also complicate the manufacturing process, seems the current sulfate level of PPS should be sufficient for clinical usage. However, despite this *in-vitro* study showed that high molecular weight PPS exert stronger effects in chondrocytes, several points need to be considered from the clinical aspect; 1. While previous findings have indicated that increased molecular size of PPS reduces its urine excretion (Erickson *et al.*, 2006), it is necessary to check if the molecular weight of PPS affects its *in-vivo* pharmacokinetics; 2. Side effects of high molecular weights

PPS. As a low-molecular-weight heparin mimic, PPS was once used for antithrombotic treatments in humans (Ghosh, 1999). Increasing the molecular weight of PPS may enhance its heparin-like properties; 3. PPS has been proved with promised anti-inflammatory properties in OA (Bwalya *et al.*, 2017a; Sunaga *et al.*, 2012), the influence of molecular weight change on these effects should be discussed. The author has found some evidence through a preliminary experiment suggested that higher molecular weights PPS could exert stronger anti-inflammatory effects in chondrocytes. Further tests need to be done before drawing a conclusion. Although the connection between its structure and effects requires further investigation, the finding of this study demonstrated that effects of PPS could be largely modulates by the variation of sulfate level and molecular weight, which provided valuable information for future pharmacological experiments and *in-vivo* tests.

Conclusion

This dissertation described structure-dependent effects of PPS in regulating canine articular chondrocytes redifferentiation and promoting the ECM synthesis of the chondrocytes through interfering the activity of Akt signaling pathway. As a DMOAD, PPS exerted a promising effect in the present study in restoring the lost phenotype of chondrocytes, which could become a potential target of interest for the development of pharmaceutical treatments of OA and other degenerative joint changes. In addition, the information about structure-effects relation of PPS could deepen our understanding about how PPS interact with the body, which would be helpful to improve the treatment effects of PPS and expand the usage of this drug. The finding of this dissertation will surely provide the information for understanding the pathogenesis of OA, and the molecular mechanisms of the therapeutic effects of PPS, which could contribute to the development of medical management of OA in research and clinical practice, and finally help to solve OA problems in animals in the future.

References

Aigner T, Söder S, Gebhard PM, McAlinden A, Haag J. 2007. Mechanisms of disease: role of chondrocytes in the pathogenesis of osteoarthritis--structure, chaos and senescence. *Nat Clin Pract Rheumatol*. **3(7)**: 391–399.

Akaraphutiporn E, Bwalya EC, Kim S, Sunaga T, Echigo R, Okumura M. 2020. Effects of pentosan polysulfate on cell proliferation, cell cycle progression and cyclin-dependent kinases expression in canine articular chondrocytes. *J Vet Med Sci*. **82(8)**: 1209–1218.

Akaraphutiporn E, Sunaga T, Bwalya EC, Echigo R, Okumura M. 2020. Alterations in characteristics of canine articular chondrocytes in non-passaged long-term monolayer culture: Matter of differentiation, dedifferentiation and redifferentiation. *J Vet Med Sci*. **82(6)**: 793–803.

Akiyama H, Lyons JP, Mori-Akiyama Y, Yang X, Zhang R, Zhang Z, Deng JM, Taketo MM, Nakamura T, Behringer RR, McCrea PD, de Crombrugghe B. 2004. Interactions between Sox9 and beta-catenin control chondrocyte differentiation. *Genes Dev*. **18(9)**: 1072–1087.

Akkiraju H, Nohe A. 2015. Role of Chondrocytes in cartilage formation, progression of osteoarthritis and cartilage regeneration. *J Dev Biol*. **3(4)**: 177–192.

Alekseeva A, Raman R, Eisele G, Clark T, Fisher A, Lee SL, Jiang X, Torri G, Sasisekharan R, Bertini S. 2020. In-depth structural characterization of pentosan polysulfate sodium complex drug using orthogonal analytical tools. *Carbohydr Polym*. **234**: 115913.

Allen JL, Cooke ME, Alliston T. 2012. ECM stiffness primes the TGFβ pathway to promote chondrocyte differentiation. *Mol Biol Cell*. **23(18)**: 3731–3742.

Anandacoomarasamy A, March L. 2010. Current evidence for osteoarthritis treatments. *Ther Adv Musculoskelet Dis*. **2(1)**: 17–28.

Anderer U, Libera J. 2002. In vitro engineering of human autogenous cartilage. *J Bone Miner Res*. **17(8)**: 1420–1429.

Archer CW, Francis-West P. 2003. The chondrocyte. *Int J Biochem Cell Biol*. **35(4)**: 401–404.

Asperti M, Denardo A, Gryzik M, Castagna A, Girelli D, Naggi A, Arosio P, Poli M. 2020. Pentosan polysulfate to control hepcidin expression in vitro and in vivo. *Biochem*

Pharmacol. **175**: 113867.

Asperti M, Naggi A, Esposito E, Ruzzenenti P, di Somma M, Gryzik M, Arosio P, Poli M. 2015. High sulfation and a high molecular weight are important for anti-hepcidin activity of heparin. *Front Pharmacol*. **6**: 316.

Bassleer C, Gysen P, Foidart JM, Bassleer R, Franchimont P. 1986. Human chondrocytes in tridimensional culture. *In Vitro Cell Dev Biol*. **22(3 Pt 1)**: 113–119.

Beier F, Leask TA, Haque S, Chow C, Taylor AC, Lee RJ, Pestell RG, Ballock RT, LuValle P. 1999. Cell cycle genes in chondrocyte proliferation and differentiation. *Matrix Biol*. **18(2)**: 109–120.

Bernstein P, Dong M, Corbeil D, Gelinsky M, Günther KP, Fickert S. 2009. Pellet culture elicits superior chondrogenic redifferentiation than alginate-based systems. *Biotechnol Prog*. **25(4)**: 1146–1152.

Berridge MJ. 2014. Module 9: Cell cycle and proliferation. *Cell Signalling Biology*. **6**: csb0001009.

Bi W, Deng JM, Zhang Z, Behringer RR, de Crombrugghe B. 1999. Sox9 is required for cartilage formation. *Nat Genet*. **22(1)**: 85–89.

Borthakur A, Mellon E, Niyogi S, Witschey W, Kneeland JB, Reddy R. 2006. Sodium and T1rho MRI for molecular and diagnostic imaging of articular cartilage. *NMR Biomed*. **19(7)**: 781–821.

Buee L, Boyle NJ, Zhang LB, Delacourte A, Fillit HM. 1991. Optimization of an alcian blue dot-blot assay for the detection of glycosaminoglycans and proteoglycans. *Anal Biochem*. **195(2)**: 238–242.

Bwalya E, Kim S, Fang J, Wijekoon HS, Hosoya K, Okumura M. 2018. Pentosan polysulfate sodium restores the phenotype of dedifferentiated monolayer canine articular chondrocytes cultured in alginate beads. *J Tissue Sci Eng*. **09(01)**: 218.

Bwalya EC, Kim S, Fang J, Wijekoon HMS, Hosoya K, Okumura M. 2017a. Pentosan polysulfate inhibits IL-1β-induced iNOS, c-Jun and HIF-1α upregulation in canine articular chondrocytes. *PLoS One*. **12(5)**: e0177144.

Bwalya EC, Kim S, Fang J, Wijekoon HMS, Hosoya K, Okumura M. 2017b. Effects of pentosan polysulfate and polysulfated glycosaminoglycan on chondrogenesis of canine

bone marrow-derived mesenchymal stem cells in alginate and micromass culture. *J Vet Med Sci*. **79(7)**: 1182–1190.

Caron JP, Genovese RL. 2003. Principles and practices of joint disease treatment. *Diagnosis and Management of Lameness in the Horse.* pp. 746–764.

Caron MMJ, Emans PJ, Coolsen MME, Voss L, Surtel DAM, Cremers A, van Rhijn LW, Welting TJM. 2012. Redifferentiation of dedifferentiated human articular chondrocytes: comparison of 2D and 3D cultures. *Osteoarthritis Cartilage*. **20(10)**: 1170–1178.

Chan DD, Li J, Luo W, Predescu DN, Cole BJ, Plaas A. 2018. Pirfenidone reduces subchondral bone loss and fibrosis after murine knee cartilage injury. *J Orthop Res*. **36(1)**: 365–376.

Charlier E, Deroyer C, Ciregia F, Malaise O, Neuville S, Plener Z, Malaise M, de Seny D. 2019. Chondrocyte dedifferentiation and osteoarthritis (OA). *Biochem Pharmacol*. **165**: 49–65.

Charlier E, Relic B, Deroyer C, Malaise O, Neuville S, Collée J, Malaise MG, de Seny D. 2016. Insights on molecular mechanisms of chondrocytes death in osteoarthritis. *Int J Mol Sci*. **17(12)**: 2146.

Chen H, Tan XN, Hu S, Liu RQ, Peng LH, Li YM, Wu P. 2021. Molecular mechanisms of chondrocyte proliferation and differentiation. *Front Cell Dev Biol*. **9**: 664168.

Chijimatsu R, Saito T. 2019. Mechanisms of synovial joint and articular cartilage development. *Cell Mol Life Sci*. **76(20)**: 3939–3952.

Dai J, Sun Y, Chen D, Zhang Y, Yan L, Li X, Wang J. 2019. Negative regulation of PI3K/AKT/mTOR axis regulates fibroblast proliferation, apoptosis and autophagy play a vital role in triptolide-induced epidural fibrosis reduction. *Eur J Pharmacol*. **864**: 172724.

Darling EM, Athanasiou KA. 2005. Rapid phenotypic changes in passaged articular chondrocyte subpopulations. *J Orthopc Res*. **23(2)**: 425–432.

Dequeker J, Luyten FP. 2008. The history of osteoarthritis-osteoarthrosis. *Ann Rheum Dis*. **67(1)**: 5–10.

Deroyer C, Charlier E, Neuville S, Malaise O, Gillet P, Kurth W, Chariot A, Malaise M, de Seny D. 2019. CEMIP (KIAA1199) induces a fibrosis-like process in osteoarthritic

chondrocytes. *Cell Death Dis*. **10(2)**: 103.

El Masri R, Seffouh A, Lortat-Jacob H, Vivès RR. 2017. The “in and out” of glucosamine 6-O-sulfation: the 6th sense of heparan sulfate. *Glycoconj J*. **34(3)**: 285–298.

Eo SH, Cho HS, Kim SJ. 2014. Resveratrol regulates type II collagen and COX-2 expression via the ERK, p38 and Akt signaling pathways in rabbit articular chondrocytes. *Exp Ther Med*. **7(3)**: 640–648.

Erickson DR, Sheykhnazari M, Bhavanandan VP. 2006. Molecular size affects urine excretion of pentosan polysulfate. *J Urol*. **175(3 Pt 1)**:1143-1147.

Esquivel CO, Bergqvist D, Björck CG, Nilsson B. 1982. Comparison between commercial heparin, low molecular weight heparin and pentosan polysulfate on hemostasis and platelets in vivo. *Thromb Res*. **28(3)**: 389–399.

Eyre D. 2002. Collagen of articular cartilage. *Arthritis Res*. **4(1)**: 30–35.

Eyre DR, Wu JJ. 1995. Collagen structure and cartilage matrix integrity. *J Rheumatol Suppl*. **43**: 82–85.

Fox AJS, Bedi A, Rodeo SA. 2009. The basic science of articular cartilage: structure, composition, and function. *Sports Health*. **1(6)**: 461–468.

Fujita T, Azuma Y, Fukuyama R, Hattori Y, Yoshida C, Koida M, Ogita K, Komori T. 2004. Runx2 induces osteoblast and chondrocyte differentiation and enhances their migration by coupling with PI3K-Akt signaling. *J Cell Biol*. **166(1)**: 85–95.

Gao Y, Liu S, Huang J, Guo W, Chen J, Zhang L, Zhao B, Peng J, Wang A, Wang Y, Xu W, Lu S, Yuan M, Guo Q. 2014. The ECM-cell interaction of cartilage extracellular matrix on chondrocytes. *Biomed Res Int*. **2014**: 648459.

García-Carvajal YZ, Garciadiego-Cázares D, Parra-Cid C, Aguilar-Gaytán R, Velasquillo C, Ibarra C, Castro Carmona JS. 2013. Cartilage tissue engineering: the role of extracellular matrix (ECM) and novel strategies. *Regenerative Medicine and Tissue Engineering*.

Gelse K, Ekici AB, Cipa F, Swoboda B, Carl HD, Olk A, Hennig FF, Klinger P. 2012. Molecular differentiation between osteophytic and articular cartilage--clues for a transient and permanent chondrocyte phenotype. *Osteoarthritis Cartilage*. **20(2)**: 162–171.

Gérard C, Goldbeter A. 2014. The balance between cell cycle arrest and cell proliferation: control by the extracellular matrix and by contact inhibition. *Interface Focus*. **4(3)**: 20130075.

Ghosh P. 1999. The pathobiology of osteoarthritis and the rationale for the use of pentosan polysulfate for its treatment. *Semin Arthritis Rheum*. **28(4)**: 211–267.

Ghosh P, Edelman J, March L, Smith M. 2005. Effects of pentosan polysulfate in osteoarthritis of the knee: A randomized, double-blind, placebo-controlled pilot study. *Curr Ther Res Clin Exp*. **66(6)**: 552–571.

Ghosh P, Wu J, Shimmon S, Zannettino AC, Gronthos S, Itescu S. 2010. Pentosan polysulfate promotes proliferation and chondrogenic differentiation of adult human bone marrow-derived mesenchymal precursor cells. *Arthritis Res Ther*. **12(1)**: R28.

Ghouri A, Conaghan PG. 2019. Update on novel pharmacological therapies for osteoarthritis. *Ther Adv Musculoskelet Dis*. **11**: 1759720X19864492.

Giovannini S, Diaz-Romero J, Aigner T, Heini P, Mainil-Varlet P, Nesic D. 2010. Micromass co-culture of human articular chondrocytes and human bone marrow mesenchymal stem cells to investigate stable neocartilage tissue formation in vitro. *Eur Cell Mater*. **20**: 245–259.

Glyn-Jones S, Palmer AJR, Agricola R, Price AJ, Vincent TL, Weinans H, Carr AJ. 2015. Osteoarthritis. *Lancet*. **386(9991)**: 376–387.

Goldring MB. 2012. Chondrogenesis, chondrocyte differentiation, and articular cartilage metabolism in health and osteoarthritis. *Ther Adv Musculoskelet Dis*. **4(4)**: 269–285.

Goldring MB, Marcu KB. 2009. Cartilage homeostasis in health and rheumatic diseases. *Arthritis Res Ther*. **11(3)**: 224.

Greco KV, Iqbal AJ, Rattazzi L, Nalesso G, Moradi-Bidhendi N, Moore AR, Goldring MB, Dell'Accio F, Perretti M. 2011a. High density micromass cultures of a human chondrocyte cell line: a reliable assay system to reveal the modulatory functions of pharmacological agents. *Biochem Pharmacol*. **82(12)**: 1919–1929.

Griffin M, Ryan CM, Pathan O, Abraham D, Denton CP, Butler PEM. 2017. Characteristics of human adipose derived stem cells in scleroderma in comparison to sex and age matched normal controls: implications for regenerative medicine. *Stem Cell Res Ther*.

8(1): 23.

Grigull NP, Redeker JI, Schmitt B, Saller MM, Schönitzer V, Mayer-Wagner S. 2020. Chondrogenic potential of pellet culture compared to high-density culture on a bacterial cellulose hydrogel. *Int J Mol Sci*. **21(8)**: 2785.

Haas S. 2003. The present and future of heparin, low molecular weight heparins, pentasaccharide, and hirudin for venous thromboembolism and acute coronary syndromes. *Semin Vasc Med*. **3(2)**: 139–146.

Hall AC. 2019. The role of chondrocyte morphology and volume in controlling phenotype-implications for osteoarthritis, cartilage repair, and cartilage engineering. *Curr Rheumatol Rep*. **21(8)**: 38.

Henrotin Y, Sanchez C, Balligand M. 2005. Pharmaceutical and nutraceutical management of canine osteoarthritis: present and future perspectives. *Vet J*. **170(1)**: 113–123.

Huang JG, Xia C, Zheng XP, Yi TT, Wang XY, Song G, Zhang B. 2011. 17β-Estradiol promotes cell proliferation in rat osteoarthritis model chondrocytes via PI3K/Akt pathway. *Cell Mol Biol Lett*. **16(4)**: 564–575.

Hunter DJ, March L, Chew M. 2020. Osteoarthritis in 2020 and beyond: a Lancet Commission. *Lancet*. **396(10264)**: 1711–1712.

Hwang HS, Lee MH, Kim HA. 2020. TGF-β1-induced expression of collagen type II and ACAN is regulated by 4E-BP1, a repressor of translation. *FASEB J*. **34(7)**: 9531–9546.

Hwang SG, Song SM, Kim JR, Park CS, Song WK, Chun JS. 2007. Regulation of type II collagen expression by cyclin-dependent kinase 6, cyclin D1, and p21 in articular chondrocytes. *IUBMB Life*. **59(2)**: 90–98.

Johnston SA. 1997. Osteoarthritis. Joint anatomy, physiology, and pathobiology. *Vet Clin North Am Small Anim Pract*. **27(4)**: 699–723.

Kapoor M. 2015. Pathogenesis of osteoarthritis. *Osteoarthritis*. pp. 1–28.

Keegan KG. 2007. Evidence-based lameness detection and quantification. *Vet Clin North Am Equine Pract*. **23(2)**: 403–423.

Kita K, Kimura T, Nakamura N, Yoshikawa H, Nakano T. 2008. PI3K/Akt signaling as a key regulatory pathway for chondrocyte terminal differentiation. *Genes Cells*. **13(8)**: 839–

850.

Krasnokutsky S, Attur M, Palmer G, Samuels J, Abramson SB. 2008. Current concepts in the pathogenesis of osteoarthritis. *Osteoarthritis Cartilage*. **16 Suppl 3**: S1-3.

Kuettner KE, Pauli BU, Gall G, Memoli VA, Schenk RK. 1982. Synthesis of cartilage matrix by mammalian chondrocytes in vitro. I. Isolation, culture characteristics, and morphology. *J Cell Biol*. **93(3)**: 743–750.

Kumagai K, Shirabe S, Miyata N, Murata M, Yamauchi A, Kataoka Y, Niwa M. 2010. Sodium pentosan polysulfate resulted in cartilage improvement in knee osteoarthritis--an open clinical trial. *BMC Clin Pharmacol*. **10(1)**: 7.

Kumar P, Nagarajan A, Uchil PD. 2018. Analysis of cell viability by the MTT assay. *Cold Spring Harb Protoc*. **2018(6)**.

Kuyinu EL, Narayanan G, Nair LS, Laurencin CT. 2016. Animal models of osteoarthritis: classification, update, and measurement of outcomes. *J Orthop Surg Res*. **11(1)**: 19.

Lefebvre V, Huang W, Harley VR, Goodfellow PN, de Crombrugghe B. 1997. SOX9 is a potent activator of the chondrocyte-specific enhancer of the pro alpha1(II) collagen gene. *Mol Cell Biol*. **17(4)**: 2336–2346.

Liang J, Xu L, Zhou F, Liu AM, Ge HX, Chen YY, Tu M. 2018. MALAT1/miR-127-5p regulates osteopontin (OPN)-mediated proliferation of human chondrocytes through PI3K/Akt pathway. *J Cell Biochem*. **119(1)**: 431–439.

Lin L, Yu Y, Zhang F, Xia K, Zhang X, Linhardt RJ. 2019. Bottom-up and top-down profiling of pentosan polysulfate. *Analyst*. **144(16)**: 4781–4786.

Lin Z, Fitzgerald JB, Xu J, Willers C, Wood D, Grodzinsky AJ, Zheng MH. 2008. Gene expression profiles of human chondrocytes during passaged monolayer cultivation. *J Orthop Res*. **26(9)**: 1230–1237.

Linhardt RJ, Toida T. 2004. Role of glycosaminoglycans in cellular communication. *Acc Chem Res*. **37(7)**: 431–438.

Liu N, Fu D, Yang J, Liu P, Song X, Wang X, Li R, Fu Z, Chen J, Gong X, Chen C, Yang L. 2020. Asiatic acid attenuates hypertrophic and fibrotic differentiation of articular chondrocytes via AMPK/PI3K/AKT signaling pathway. *Arthritis Res Ther*. **22(1)**: 112.

Loeser RF, Goldring SR, Scanzello CR, Goldring MB. 2012. Osteoarthritis: a disease of the joint as an organ. *Arthritis Rheum*. **64(6)**: 1697–1707.

Maldonado M, Nam J. 2013. The role of changes in extracellular matrix of cartilage in the presence of inflammation on the pathology of osteoarthritis. *Biomed Res Int*. **2013**: 284873.

Mao Y, Hoffman T, Wu A, Kohn J. 2018. An innovative laboratory procedure to expand chondrocytes with reduced dedifferentiation. *Cartilage*. **9(2)**: 202–211.

McIlwraith CW, Frisbie DD, Kawcak CE. 2012. Evaluation of intramuscularly administered sodium pentosan polysulfate for treatment of experimentally induced osteoarthritis in horses. *Am J Vet Res*. **73(5)**: 628–633.

Medvedeva E v, Grebenik EA, Gornostaeva SN, Telpuhov VI, Lychagin A v, Timashev PS, Chagin AS. 2018. Repair of damaged articular cartilage: current approaches and future directions. *Int J Mol Sci*. **19(8)**: 2366.

Meneghetti MCZ, Hughes AJ, Rudd TR, Nader HB, Powell AK, Yates EA, Lima MA. 2015. Heparan sulfate and heparin interactions with proteins. *J R Soc Interface*. **12(110)**: 0589.

Merceron C, Portron S, Vignes-Colombeix C, Rederstorff E, Masson M, Lesoeur J, Sourice S, Sinquin C, Colliec-Jouault S, Weiss P, Vinatier C, Guicheux J. 2012. Pharmacological modulation of human mesenchymal stem cell chondrogenesis by a chemically oversulfated polysaccharide of marine origin: potential application to cartilage regenerative medicine. *Stem Cells*. **30(3)**: 471–480.

Mhanna R, Kashyap A, Palazzolo G, Vallmajo-Martin Q, Becher J, Möller S, Schnabelrauch M, Zenobi-Wong M. 2014. Chondrocyte culture in three dimensional alginate sulfate hydrogels promotes proliferation while maintaining expression of chondrogenic markers. *Tissue Eng Part A*. **20(9–10)**: 1454–1464.

Mizumoto S, Yamada S, Sugahara K. 2015. Molecular interactions between chondroitin-dermatan sulfate and growth factors/receptors/matrix proteins. *Curr Opin Struct Biol*. **34**: 35–42.

Mobasheri A. 2013. The future of osteoarthritis therapeutics: targeted pharmacological therapy. *Curr Rheumatol Rep*. **15(10)**: 364.

Mora JC, Przkora R, Cruz-Almeida Y. 2018. Knee osteoarthritis: pathophysiology and

current treatment modalities. *J Pain Res*. **11**: 2189–2196.

Mousa SA. 2005. Effect of low molecular weight heparin and different heparin molecular weight fractions on the activity of the matrix-degrading enzyme aggrecanase: structure-function relationship. *J Cell Biochem*. **95(1)**: 95–98.

Neogi T. 2013. The epidemiology and impact of pain in osteoarthritis. *Osteoarthritis Cartilage*. **21(9)**: 1145–1153.

Nurse P. 2000. The incredible life and times of biological cells. *Science*. **289(5485)**: 1711–1716.

O'Neill DG, Church DB, McGreevy PD, Thomson PC, Brodbelt DC. 2014. Prevalence of disorders recorded in dogs attending primary-care veterinary practices in England. *PLoS One*. **9(3)**: e90501.

Oo WM, Hunter DJ. 2022. Repurposed and investigational disease-modifying drugs in osteoarthritis (DMOADs). *Ther Adv Musculoskelet Dis*. **14**: 1759720X221090297.

Oo WM, Little C, Duong V, Hunter DJ. 2021. The development of disease-modifying therapies for osteoarthritis (DMOADs): the evidence to date. *Drug Des Devel Ther*. **15**: 2921–2945.

Ori A, Wilkinson MC, Fernig DG. 2011. A systems biology approach for the investigation of the heparin/heparan sulfate interactome. *J Biol Chem*. **286(22)**: 19892–19904.

Otero M, Favero M, Dragomir C, Hachem KE, Hashimoto K, Plumb DA, Goldring MB. 2012. Human chondrocyte cultures as models of cartilage-specific gene regulation. *Methods Mol Biol*. 806: 301–336.

Palhares LCGF, London JA, Kozlowski AM, Esposito E, Chavante SF, Ni M, Yates EA. 2021. Chemical modification of glycosaminoglycan polysaccharides. *Molecules*. **26(17)**: 5211.

Park JS, Woo DG, Yang HN, Lim HJ, Chung HM, Park KH. 2008. Heparin-bound transforming growth factor-beta3 enhances neocartilage formation by rabbit mesenchymal stem cells. *Transplantation*. **85(4)**: 589–596.

Parrales A, López E, López-Colomé AM. 2011. Thrombin activation of PI3K/PDK1/Akt signaling promotes cyclin D1 upregulation and RPE cell proliferation. *Biochim Biophys Acta*. **1813(10)**: 1758–1766.

Parreno J, Nabavi Niaki M, Andrejevic K, Jiang A, Wu P-H, Kandel RA. 2017. Interplay between cytoskeletal polymerization and the chondrogenic phenotype in chondrocytes passaged in monolayer culture. *J Anat*. **230(2)**: 234–248.

Parsons CL, Benson G, Childs SJ, Hanno P, Sant GR, Webster G. 1993. A quantitatively controlled method to study prospectively interstitial cystitis and demonstrate the efficacy of pentosanpolysulfate. *J Urol*. **150(3)**: 845–848.

Pearle AD, Warren RF, Rodeo SA. 2005. Basic science of articular cartilage and osteoarthritis. *Clin Sports Med*. **24(1)**: 1–12.

Qu Z, Weiss JN, MacLellan WR. 2003. Regulation of the mammalian cell cycle: a model of the G1-to-S transition. *Am J Physiol Cell Physiol*. **284(2)**: C349-C364.

Ripmeester EGJ, Timur UT, Caron MMJ, Welting TJM. 2018. Recent insights into the contribution of the changing hypertrophic chondrocyte phenotype in the development and progression of osteoarthritis. *Front Bioeng Biotechnol*. **6**: 18.

Rosenberg RD, Lam L. 1979. Correlation between structure and function of heparin. *Proc Natl Acad Sci U S A*. **76(3)**: 1218–1222.

Roughley PJ, Lee ER. 1994. Cartilage proteoglycans: structure and potential functions. *Microsc Res Tech*. **28(5)**: 385–397.

San Antonio JD, Winston BM, Tuan RS. 1987. Regulation of chondrogenesis by heparan sulfate and structurally related glycosaminoglycans. *Dev Biol*. **123(1)**: 17–24.

Sandell LJ, Aigner T. 2001. Articular cartilage and changes in arthritis. An introduction: cell biology of osteoarthritis. *Arthritis Res*. **3(2)**: 107–113.

Sanden C, Mori M, Jogdand P, Jönsson J, Krishnan R, Wang X, Erjefält JS. 2017. Broad Th2 neutralization and anti-inflammatory action of pentosan polysulfate sodium in experimental allergic rhinitis. *Immun Inflamm Dis*. **5(3)**: 300–309.

Sanderson RO, Beata C, Flipo RM, Genevois JP, Macias C, Tacke S, Vezzoni A, Innes JF. 2009. Systematic review of the management of canine osteoarthritis. *Vet Rec*. **164(14)**: 418–424.

Shah K, Drury T, Roic I, Hansen P, Malin M, Boyd R, Sumer H, Ferguson R. 2018. Outcome of allogeneic adult stem cell therapy in dogs suffering from osteoarthritis and other joint defects. *Stem Cells Int*. **2018**: 1–7.

Singh P, Marcu KB, Goldring MB, Otero M. 2019. Phenotypic instability of chondrocytes in osteoarthritis: on a path to hypertrophy. *Ann N Y Acad Sci*. **1442(1)**: 17–34.

Sokolove J, Lepus CM. 2013. Role of inflammation in the pathogenesis of osteoarthritis: latest findings and interpretations. *Ther Adv Musculoskelet Dis*. **5(2)**: 77–94.

Sunaga T, Oh N, Hosoya K, Takagi S, Okumura M. 2012. Inhibitory effects of pentosan polysulfate sodium on MAP-Kinase pathway and NF-κB nuclear translocation in canine chondrocytes in vitro. *J Vet Med Sci*. **74(6)**: 707–711.

Sylvester PW. 2011. Optimization of the tetrazolium dye (MTT) colorimetric assay for cellular growth and viability. *Methods Mol Biol*. **716**: 157–168.

Takahashi I, Nuckolls GH, Takahashi K, Tanaka O, Semba I, Dashner R, Shum L, Slavkin HC. 1998. Compressive force promotes sox9, type II collagen and aggrecan and inhibits IL-1beta expression resulting in chondrogenesis in mouse embryonic limb bud mesenchymal cells. *J Cell Sci*. **111(Pt 14)**: 2067–2076.

Tao H, Cheng L, Yang R. 2020. Downregulation of miR-34a promotes proliferation and inhibits apoptosis of rat osteoarthritic cartilage cells by activating PI3K/Akt pathway. *Clin Interv Aging*. **15**: 373–385.

Taruc-Uy RL, Lynch SA. 2013. Diagnosis and treatment of osteoarthritis. *Prim Care*. **40(4)**: 821–836, vii.

Thompson LD, Pantoliano MW, Springer BA. 1994. Energetic characterization of the basic fibroblast growth factor-heparin interaction: identification of the heparin binding domain. *Biochemistry*. **33(13)**: 3831–3840.

Thonar EJ, Buckwalter JA, Kuettner KE. 1986. Maturation-related differences in the structure and composition of proteoglycans synthesized by chondrocytes from bovine articular cartilage. *J Biol Chem*. **261(5)**: 2467–2474.

Troeberg L, Fushimi K, Khokha R, Emonard H, Ghosh P, Nagase H. 2008. Calcium pentosan polysulfate is a multifaceted exosite inhibitor of aggrecanases. *FASEB J*. **22(10)**: 3515–3524.

Troeberg L, Mulloy B, Ghosh P, Lee MH, Murphy G, Nagase H. 2012. Pentosan polysulfate increases affinity between ADAMTS-5 and TIMP-3 through formation of an electrostatically driven trimolecular complex. *Biochem J*. **443(1)**: 307–315.

Tsogbadrakh M, Sunaga T, Bwalya E, Wijekoon S, Akaraphutiporn E, Wang Y, Mwale C, Naranbaatar A, Kim S, Hosoya K, Alimaa D, Okumura M. 2020. Clinical evaluation of pentosan polysulfate as a chondroprotective substance in native mongolian horses. *Jpn J Vet Res*. **68(3)**: 203–208.

Ulici V, Hoenselaar KD, Gillespie JR, Beier F. 2008. The PI3K pathway regulates endochondral bone growth through control of hypertrophic chondrocyte differentiation. *BMC Dev Biol*. **8(1)**: 40.

Ophoven VA, Vonde K, Koch W, Auerbach G, Maag KP. 2019. Efficacy of pentosan polysulfate for the treatment of interstitial cystitis/bladder pain syndrome: results of a systematic review of randomized controlled trials. *Curr Med Res Opin*. **35(9)**: 1495–1503.

Wang Z, Zhang F, S. Dordick J, J. Linhardt R. 2012. Molecular Mass Characterization of glycosaminoglycans with different degrees of sulfation in bioengineered heparin process by size exclusion chromatography. *Curr Anal Chem*. **8(4)**: 506–511.

Watt FM. 1988. Effect of seeding density on stability of the differentiated phenotype of pig articular chondrocytes in culture. *J Cell Sci*. **89(Pt 3)**: 373–378.

Weinstein AM, Rome BN, Reichmann WM, Collins JE, Burbine SA, Thornhill TS, Wright J, Katz JN, Losina E. 2013. Estimating the burden of total knee replacement in the United States. *J Bone Joint Surg Am*. **95(5)**: 385–392.

Wu J, Shimmon S, Paton S, Daly C, Goldschlager T, Gronthos S, Zannettino ACW, Ghosh P. 2017. Pentosan polysulfate binds to STRO-1+ mesenchymal progenitor cells, is internalized, and modifies gene expression: a novel approach of pre-programing stem cells for therapeutic application requiring their chondrogenesis. *Stem Cell Res Ther*. **8(1)**: 278.

Xu D, Esko JD. 2014. Demystifying heparan sulfate-protein interactions. *Annu Rev Biochem*. **83**: 129–157.

Yang C, Cao M, Liu H, He Y, Xu J, Du Y, Liu Y, Wang W, Cui L, Hu J, Gao F. 2012. The high and low molecular weight forms of hyaluronan have distinct effects on CD44 clustering. *J Biol Chem*. **287(51)**: 43094–43107.

Yeung P, Cheng KH, Yan CH, Chan BP. 2019. Collagen microsphere based 3D culture

system for human osteoarthritis chondrocytes (hOACs). *Sci Rep*. **9(1)**: 12453.

Yu SP, Hunter DJ. 2015. Managing osteoarthritis. *Aust Prescr*. **38(4)**: 115–119.

Zaucke F, Dinser R, Maurer P, Paulsson M. 2001. Cartilage oligomeric matrix protein (COMP) and collagen IX are sensitive markers for the differentiation state of articular primary chondrocytes. *Biochem J*. **358(Pt 1)**: 17–24.

Abstract of the Dissertation

Structure-related effects of pentosan polysulfate sodium: modulation on phenotypic change and chondrogenic properties in canine chondrocyte *in-vitro* cultures

Hyaline cartilage is a specialized connective tissue on the joint surface that supports normal joint movements and protects the subchondral bone. Chondrocytes are the only cellular components in the cartilage, which are physiologically responsible for maintaining a balance between the synthesis and degradation of the extracellular matrix (ECM). Osteoarthritis (OA) is the most common degenerative joint disease that progressively destroys the joint structures, including cartilages. During OA pathogenesis, chondrocytes undergo a dedifferentiated phenotypic change that leads to transiently increased proliferation, downregulated ECM biosynthesis, and activated production of biochemical mediators associated with OA progression. These changes of chondrocytes disturbed cartilage homeostasis, which pharmacological interventions of chondrocytes dedifferentiation could be beneficial for OA treatment.

Pentosan polysulfate sodium (PPS) is a semi-synthetic polysaccharide, which has been found to relieve OA symptoms in animals. Although the underlying mechanisms are not fully understood, PPS has shown effects in promoting the redifferentiation and ECM production of articular chondrocytes. On the other hand, the structure similarity between PPS and glycosaminoglycans has been identified. Since glycosaminoglycans achieve their biological properties mainly through the interaction with proteins, modifying their molecular weights or sulfate levels could alter their effects. However, the structure-effect relation of PPS is rarely discussed. To improve the therapeutic effects of PPS, more information is need.

Therefore, the present study was conducted with two major objectives: 1. To check the effects on the phenotypic changes and ECM production of dedifferentiated canine chondrocytes and the underlying molecular mechanisms of these effects. 2. To explore how the variations in molecular weights and sulfate levels of PPS affect these treatment effects.

This dissertation contains two sections: Section one investigated the effects of different sulfate levels PPS on the proliferation and cell cycle in dedifferentiated chondrocytes and the related phenotypic change in monolayer cultures. In the second section, the effects in promoting the redifferentiation and ECM production of canine chondrocytes were further investigated in micro-mass cultures using PPS with different molecular weights.

The results of this study provide evidence that PPS exerts inhibitory effects on cell cycle progression while promotes the redifferentiation of dedifferentiated canine articular chondrocytes in monolayer cultures, which involves the suppression of PI3K/Akt signaling pathway. The improvement in the phenotype and ECM production of chondrocytes with PPS treatment was further confirmed under a micro-mass cultured condition. Relations between the structure and the anabolic effects of PPS was also confirm in this study, which larger PPS molecules (5,000 and 7,000 Da) exert stronger effects in promoting chondrocyte redifferentiation and ECM synthesis. Furthermore, the full sulfate level of PPS seems to be necessary to achieve these effects.

In conclusion, this dissertation provided further information on the therapeutic effects of PPS in canine articular chondrocytes and their underlying mechanisms, which could be a potential target for developing pharmaceutical treatments for OA. In addition, the information about structure-effects relation of PPS could deepen the understanding of its interaction with the body and help to improve the treatment effects of PPS, which would have a positive impact to solve OA problems in animals.

Acknowledgements

The completion of this thesis could not have been possible without the scientific support and enthusiastic assistance of many people.

First and foremost, I would like to convey my deep and sincere gratitude to Prof. Masahiro Okumura, my supervisor, for giving me an opportunity to start my work associated with doctoral studies in the Laboratory of Veterinary Surgery, Graduate School of Veterinary Medicine, Hokkaido University and for making this research possible with his extensive knowledge, sincere and solid advice, patience, and support over the past few years.

I wish to express my deep acknowledgment to my co-advisors and thesis committee: Prof. Takashi Kimura, Associate Prof. Osamu Ichii, and Assistant Prof. Takafumi Sunaga for their brilliant comments, incisive questions which enlighten me to broaden my perspective on the research, and encouragement. I would like to sincerely thank Assistant Prof. Sangho Kim for the immeasurable supports in research materials and his scientific advice.

I would like to offer my special thanks to Dr. Ekkapol Akaraphutiporn for his persistent help for me to get adjusted to the doctoral course and keep going forward, Dr. Eugene Bwalya and Suranji Wijekoon for their advice and constructive comments on my research. Also, my sincere thanks go to all of my laboratory colleagues, Dr. Mijiddorj Tsogbadrakh, Yusuke Murase, Koangyong Sung, Takachika Sato, Carol Mwale, Ryo Owaki, Yingyuan Hsu, Kanittha Darawiroj, Nomsa Mulenga, Mika Sumita, and Nanami Maeda for their invaluable support and wonderful friendship during my study in the Laboratory of Veterinary Surgery.

My great acknowledgments to Hokkaido University DX Doctoral Fellowship and WISE program for their financial contribution during my stay at Hokkaido University. In addition, I am thankful to all staffs of the WISE program office and academic affair section for all the support during my PhD program.

Finally, I sincerely acknowledge to my parents, Xuejun Wang and Songjuan Xie, and my best friends for their support and encouragement throughout my life. Last but not least, I

would like to thank Peng Zhao for all her love, encouragement, and support. This accomplishment would not have been possible without them.

Hokkaido University, 2023

Dr. Yanlin Wang